



Cite this: *Mol. Syst. Des. Eng.*, 2020, 5, 49

# Nanomaterials for molecular signal amplification in electrochemical nucleic acid biosensing: recent advances and future prospects for point-of-care diagnostics

Léonard Bezinge, Akkapol Suea-Ngam, Andrew J. deMello \* and Chih-Jen Shih \*

With the increasing importance of personalized medicine and genomics, biosensors have received considerable attention in various fields, including clinical diagnostics, food inspection and environmental monitoring. In particular, advances in electrochemical biosensing technologies for clinical diagnostics pave the way for ultrasensitive detection of nucleic acid sequences using miniaturized and low-cost devices suitable for point-of-use applications. This account reviews three major amplification strategies utilizing nanomaterials as (i) 'nanocatalysts' in electrocatalysis, (ii) redox active reporters ('nanoreporters') and (iii) cargos for redox markers ('nanocarriers'). In addition, and motivated by the need for reproducible and robust sensing, the integration of biosensors with microfluidic tools, including paper-based devices, are also covered.

Received 1st October 2019,  
Accepted 8th November 2019

DOI: 10.1039/c9me00135b

rsc.li/molecular-engineering

## Design, System, Application

Electrochemical biosensors most usually leverage the detection of an electroactive reporter molecule to generate an analytically useful electrical signal. The sensitivity and detection limits of such sensors directly depend on the number of redox reporters that can be detected at the electrode. To detect the low (mass and concentration) levels of biomarkers in clinical samples, amplification strategies are used to increase the number of detectable molecules. In this respect, nanomaterials, due to their small size, can be used to label biomolecules and amplify the number of redox reporters. In particular, functional nanomaterials can be engineered to interact with specific nucleic acid strands and subsequently amplify associated electrochemical signals, paving the way towards robust and ultrasensitive methods for pathogen detection and disease diagnostics.

## 1. Introduction

Advances in nanotechnology have defined a step change in analytical chemistry. Owing to their high surface-to-volume ratios, nanomaterials exhibit unique physicochemical properties that differ from their bulk counterparts, providing opportunities for improved biosensing.<sup>1</sup> For example, gold nanoparticles, which appear intense red due to the plasmonic effects, have found significant commercial success as colorimetric labels in one of the most established diagnostic tests: the home urinary pregnancy test.<sup>2</sup> In many ways, they represent the 'gold standard' in rapid diagnostic tests with colorimetric readouts, and have also been used to detect various infectious diseases, such as malaria; with over 276 million tests being sold in 2017.<sup>3</sup> However, such tests provide qualitative or at best semi-quantitative readouts.

Accordingly, electrochemical biosensors have emerged as promising platforms for miniaturized devices and quantitative analyte detection. Since the first demonstration of an electrochemical glucose sensor in 1962 by Clark and Lyons,<sup>4</sup> glucose sensors have become the tool of reference for quantitative and low-cost diabetes monitoring. Indeed, as the field of diagnostics moves towards personalized medicine and molecular diagnostics, biosensors with defined specificity and high analytical sensitivity are essential to detect nucleic acids (NAs) at femto- and atto-molar concentrations in clinical samples. To this end, the development of amplification methods, involving either the multiplication of the target NAs (as in the case of polymerase chain reaction – PCR) or the amplification of biosensor signal itself, becomes critical.

Nanomaterials, due to their multifunctional nature, have facilitated the improvement of several key features in electrochemical bioassays, including sample pretreatment,<sup>5</sup> analyte capture,<sup>6</sup> signal amplification<sup>7</sup> and transduction.<sup>8</sup> Widely investigated as electrode modifiers to improve

Institute for Chemical and Bioengineering, Department of Chemistry and Applied Biosciences, ETH Zürich, Vladimir-Prelog-Weg 1, 8093 Zürich, Switzerland.  
E-mail: andrew.demello@chem.ethz.ch, chih-jen.shih@chem.ethz.ch



bioreceptor immobilization and charge transport properties,<sup>9</sup> nanomaterials have also demonstrated their potential to amplify electrochemical signals by generating increased numbers of electroactive reporters. Herein, we review recent advances in nanomaterial-based amplification strategies for electrochemical signaling, with a focus on nucleic acid detection for point-of-care diagnosis.



Léonard Bezinge

*Léonard Bezinge obtained his BSc and MSc in Chemical and Bioengineering from ETH Zurich in 2017, with a master thesis on the synthesis of fluorescent nanoparticles in microreactors. He then did an internship at the London Center for Nanotechnology (UCL) as part of the i-sense research program on the development of nanomaterials for ultrasensitive point-of-care tests. In 2019, he started his PhD studies under*

*the supervision of Prof. Shih and Prof. deMello at ETH Zurich. His current research interests focus on the development of paper-based electrochemical biosensors for rapid diagnostic testing.*

## 2. Nucleic acids as biorecognition elements

Bacterial diseases (such as tuberculosis) and their antimicrobial resistance to common antibiotics, such as penicillin, amoxicillin and erythromycin, represent a critical threat to global health<sup>10</sup> and can effectively be identified by



Akkapol Suea-Ngam

*Akkapol Suea-Ngam completed his undergraduate degree in chemistry from Chulalongkorn University, receiving the best Bachelor thesis and the Hitachi Trophy 2014 awards. He received his Masters degree in Analytical Chemistry from same department, having also spent a five month period in the Furutani group at the IMS in Japan, and was the recipient of the best Master Research Award. Thereafter, he also received*

*Ratchdapiseksompotch as the best Master Thesis Award from Chulalongkorn University. Akkapol joined the deMello group in 2016, and was the recipient of a Swiss Government Excellence Scholarship. He has experience in developing electrochemical detectors for droplet-based and paper-based microfluidic systems.*



Andrew J. deMello

*Andrew J. deMello is Professor of Biochemical Engineering in the Department of Chemistry and Applied Biosciences at ETH Zürich and Head of the Institute for Chemical and Bioengineering. Previously he was Professor of Chemical Nanosciences in the Chemistry Department at Imperial College London. His group's research interests cover a broad range of activities in the general area of microfluidics and nanoscale*

*science. Primary specializations include the development of microfluidic devices for high-throughput biological and chemical analysis, ultra-sensitive optical detection techniques, imaging flow cytometry, novel methods for nanoparticle synthesis, the exploitation of semiconducting materials in diagnostic applications and the development of intelligent microfluidic systems.*



Chih-Jen Shih

*Chih-Jen Shih has been a tenure-track assistant professor of chemical engineering at the Department of Chemistry and Applied Biosciences, ETH Zurich since 2015. He was trained in Stanford University (Postdoc, 2014–2015) and Massachusetts Institute of Technology (PhD, 2009–2014). His research group focuses on morphology, dynamics, molecular forces, and transport phenomena at nanomaterials interfaces. His*

*interest ranges from fundamental understanding of how dielectric screening of atomically thin nanomaterials influences the movement and interactions of charges, excitons, and molecules near interfaces, to application-motivated studies aimed at developing new engineering strategies to control over the interplay of these mechanisms, towards new technological opportunities in optoelectronics, sensors, and actuators. His research has been recognized by the Victor K. LaMer Award from the American Chemical Society, the Ruzicka Prize from the Swiss Chemical Society, and the ERC Starting Grant from the European Union.*



genetically detecting the antibiotic resistome (antibiotic resistance genes).<sup>11</sup> Aside from the direct genomic detection of pathogens, microRNAs (miRNAs), the short non-coding RNAs involved in gene regulation, have also been found to be promising biomarkers for cancers and infectious diseases, through their role in cellular expression during infection.<sup>12–14</sup> The highly specific properties of NA hybridization constitute a fundamental principle of DNA biosensors (genosensors), and as such enable the detection of sequence-specific NA probes with high selectivity.<sup>15</sup> In addition to DNA and RNA, other synthetic NA structures with distinct backbone properties – such as peptide nucleic acids (PNA) that possess amino acid-based backbones with neutral overall net charge and locked nucleic acid (LNA) containing a methylene bridge – have shown improvements in hybridization with target (natural) nucleic acids.<sup>16,17</sup> Synthetic NAs not only possess high binding affinities to DNA and RNA (quantified by  $K_D$ ), but are robust and allow the detection of single-base-pair mismatches.<sup>18</sup> Accordingly, the development of DNA-based sensors benefits a broad spectrum of analytical applications, including the detection of small molecules and proteins *via* SELEX-based aptamer recognition,<sup>19,20</sup> DNA-processing enzyme activity,<sup>21</sup> DNA damage<sup>22</sup> and heavy metals ion analysis.<sup>23</sup>

It is well-recognized that PCR remains the gold-standard method for DNA amplification in both laboratory and clinical settings, allowing exponential amplification of DNA *via* well-established protocols. More recently, isothermal amplification methods, such as loop mediated isothermal amplification (LAMP), recombinase polymerase amplification (RPA) and rolling circle amplification (RCA), have become increasingly important, and facilitate the development of NA assays applicable for remote-field testing.<sup>24</sup> Each of these methods has particular advantages and drawbacks, with all requiring bespoke optimization (of primer sequences, reaction concentration and reaction temperatures) to minimize non-specific amplification. Moreover, the use of NA amplification methods for diagnostics requires that biosensors can determine the presence or concentration of amplicons, either in real time or at the endpoint. Additionally, the integration of signal amplification strategies further improves the sensitivity of the assays.<sup>7</sup> Put simply, the direct detection of NA in clinical samples demands not only high sensitivity but also stringent specificity, to ensure

discrimination of the target from a heterogeneous collection of other sequences present in the sample matrix. To this end, recent efforts have focused on the development of ultrasensitive biosensors that offer robust yet flexible approaches for NA detection in resource-limited settings.<sup>25</sup>

### 3. Electrochemical sensors for nucleic acid detection

#### 3.1 Electrochemical methods

In recent decades, we have witnessed tremendous development of electrochemical biosensors as miniaturized and low-cost platforms for the rapid and sensitive detection of biomolecules. The basic principle of electrochemical detection relies on the transduction of an electrical signal, *via* a change in current, potential, accumulated charge or impedance, triggered by the recognition of a target biomolecular analyte (Fig. 1).<sup>26</sup> Accordingly, a number of electrochemical techniques have been employed for the signal characterization and quantification; predominantly amperometry, linear sweep voltammetry (LSV), cyclic voltammetry (CV), differential pulse voltammetry (DPV), square wave voltammetry (SWV), and electrochemical impedance spectroscopy (EIS). In particular, pulse methods based on voltammetry, such as DPV and SWV, have been recognized to be amongst the most sensitive approaches for quantitative analysis, allowing the differentiation of both promptly decayed charging current and the faradic current with short measurement times.<sup>27,28</sup> These methods however require system-specific optimization to maximize the signal gain, by tuning the pulse amplitude, frequency, and sampling time.<sup>29</sup>

#### 3.2 Electron transport through DNA

The detection of NA sequences generally relies on the hybridization of a target sequence with an immobilized capture probe. For example, the self-assembly of thiolated ssDNA monolayers (SAMs) on gold has been extensively used to functionalize gold electrodes with well-controlled packing densities.<sup>30</sup> However, the interaction between gold and thiolated ssDNA limits the operating potential window within  $\pm 0.6$  V with reference to Ag/AgCl at pH 7, in order to prevent the reductive desorption of thiolated ssDNA and oxidation of

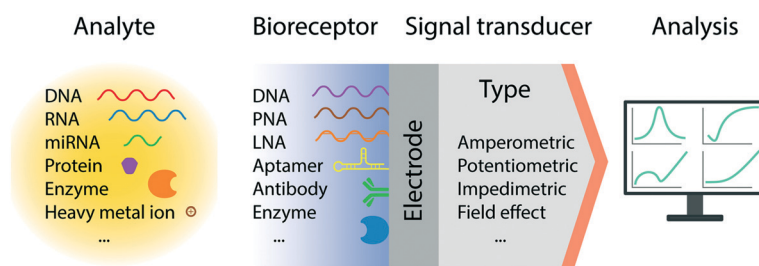


Fig. 1 Schematic representation of the general architecture of an electrochemical biosensor. The sensor consists of an integrated receptor-transducer device capable of providing analytical information based on a biological recognition element.



guanine nucleobase and thiol groups.<sup>17,31</sup> Alternatively, a robust way of immobilizing ssDNA on an electrode is to take advantage of the rapid and strong biotin–avidin interaction by attaching biotinylated ssDNA to a streptavidin-covered electrode surface.<sup>32</sup> While the conformation of ssDNA strands exhibits mechanical flexibility, double-stranded (ds) DNA possesses a rigid rod-like behaviour, capable of bending towards the electrode surface. dsDNA also mediate electron transfer through its structure,<sup>33</sup> effectively acting as an extended nanoelectrode.<sup>34,35</sup> Actually, at the current time, the mechanisms behind the DNA-mediated charge transport remain controversial.<sup>36,37</sup> For example, a number of theories have been proposed based on the long-range charge transport through the  $\pi$ – $\pi$  stacking of nucleotide orbitals mediated by the oxidation of guanine.<sup>35</sup> Conversely, Plaxco and co-workers have suggested that electrons are not transferred through the DNA strands themselves but through a contact-mediated mechanism, with the DNA duplexes bent towards the electrode surface. These claims have been supported by experiments in which guanine content, base mismatches and dsDNA probe lengths are varied.<sup>37</sup>

### 3.3 Thermodynamic and diffusion limitations

Since targets are often at ultra-low concentrations (down to the single molecule level), the thermodynamics of binding affinity must also be considered; specifically in regard to the  $k_{\text{on}}$  and  $k_{\text{off}}$  of the biomolecular interaction. Indeed, the sensor response will not reflect the measurement of an ensemble of bound molecules but is triggered by individual binding events.<sup>38,39</sup> Accordingly, the measurement time plays a crucial role when probing ultra-low concentrations, as this will be strongly influenced by the surface coverage of analytes and the capturing elements on the surfaces. Calculations by Sheehan and Whitman<sup>40</sup> suggest that concentration detection limits within the femtomolar range are limited by mass transport, which may require hours or even days for the analyte molecules to diffuse to the electrode surface.<sup>41</sup> However, this suggestion has been challenged by recent reports claiming sub-femtomolar detection limits,<sup>42</sup> and is most likely due to inconsistent definitions of detection time scales in the theoretical and experimental frameworks.<sup>43</sup> Specifically, it has been suggested that theoretical approaches actually model the mean diffusion time for an analyte to the electrode, whereas in practice, the sensor response corresponds to the minimum diffusion time that generates a detectable signal (from the tail of the statistical distribution of Brownian motion).<sup>43</sup> Furthermore, it should be remembered that a number of experimental techniques can overcome mass transport limitations, including sample pre-concentration using magnetic beads or flow-based assays that will be discussed later. Finally, reaction volumes must also be taken into account, since reductions in volume will decrease diffusion times but will also lower the mass of analyte. In this regard, one may quantitatively analyse such an issue

through estimation of the Damköhler number, which relate reaction and mass transport time scales.<sup>44</sup>

### 3.4 Electrochemical detection of DNA

Early electrochemical approaches for the detection of nucleic acids involved the inherent electroactivity of nucleotide bases *via* either reduction or oxidation pathways.<sup>45,46</sup> For example, the use of reduced graphene oxide (rGO) as an electrode material enables the detection of the four specific nucleobases within a potential window of 0.5–1.5 V *vs.* Ag/AgCl under physiological conditions, and lower than their traditional oxidative potentials.<sup>47</sup> It should be noted that the redox potentials strongly depend on the properties of the electrode surface and history of pre-treatment. Nevertheless, nucleobase oxidation peaks are relatively weak and overlap with those of water oxidation, thereby limiting the scope of such approaches for biosensors.

Hybridization-based approaches later emerged for the detection of specific NA sequences by utilizing specific physical and electrical properties of ss- and dsDNA.<sup>17</sup> In these systems, redox indicators capable of reporting the presence of hybridized probes on the electrode have attracted considerable attention.<sup>48</sup> In particular, the ferro-/ferricyanide anion couple ( $[\text{Fe}(\text{CN})_6]^{3-/-4-}$ ) has become one of the most widely used redox indicators due to its sensitivity to surface coverage.<sup>48</sup> The presence of negatively charged duplex DNAs on the surface reduces the voltammetric redox signal, which enables the quantification of hybridized targets.<sup>48</sup> As an alternative redox marker, the hexaaminoruthenium(III) ion (RuHex,  $[\text{Ru}(\text{NH}_3)_6]^{3+/2+}$ ) binds to the phosphate backbone of nucleic acids, forming conductive wires that generates electrochemical signals proportional to the amount of nucleic acids adjacent to the electrode surface.<sup>17,48</sup> The formation of molecular wires can be used in combination with other redox labels, which increases the signal by up to 5-fold,<sup>49</sup> *via* electron transfer from the DNA layer to the electrode through the inner Helmholtz plane (IHP).<sup>26</sup> There are two main types of electroactive species; inner sphere redox probes (*e.g.* ferro-/ferricyanide and dopamine) that require direct contact with the electrode surface, and outer sphere redox probes (*e.g.* RuHex) that transfer electrons over short distances (within 2–3 Å) to the electrode *via* electron tunneling.<sup>26</sup> Inner sphere redox probes are much more sensitive to the electrode surface chemistry than outer sphere probes.<sup>26</sup> Alternatively, duplex-specific redox indicators, such as methylene blue (MB), can intercalate into dsDNA strands to allow the specific detection of hybridized probes.<sup>17</sup> MB is also known to covalently link to the end of hairpin probes that are tethered on the electrode, building switchable DNA architectures labelled with a redox indicator.<sup>50</sup>

Due to the fact that clinical samples are highly heterogeneous, molecular diagnostic methods strongly benefit from molecular signal amplification methods. Inspired by the standard enzyme-linked immunosorbent assay (ELISA), electrochemical equivalents, namely, electrochemical ELISA or E-ELISA, hold promise towards



ultrasensitive detection of nucleic acids.<sup>51</sup> Such an approach uses an enzyme label in a sandwich assay to amplify reporter molecules, in which the target NA is immobilized on a transducer substrate by a capture probe, followed by tagging with a label. Together with the rise of nanotechnology, a range of novel strategies have emerged to amplify electrochemical signals.<sup>7</sup> We now review the development of nanomaterial-based signal amplification techniques.

## 4. Nanomaterials for molecular signal amplification

An important feature of a nanomaterials-based biosensing platform is that it is able to amplify electrochemical signals under mild conditions, *i.e.* at lower oxidation potentials when compared to the direct oxidation of nucleobases, by generating electroactive species that subsequently produce detectable redox events on the electrode surface. Nanoparticles normally act as labels for captured nucleic acids, either through specific interactions, such as DNA hybridization or aptamer recognition, or non-specifically, such as electrostatic or  $\pi$ - $\pi$  interactions.<sup>7</sup> Alternatively, “triggerable” amplification approaches, in which the presence of target NAs initiates the amplification activity of a freely-diffusing nanomaterial, have also been reported. In the current discussion, and as illustrated in Fig. 2, amplification strategies are categorized on the basis of the role of the nanomaterial, namely, nanocatalysts (where nanomaterials act as catalysts that facilitate the production of electroactive species), nanoreporters (where the nanomaterials themselves act as redox active species) and nanocarriers (where the nanomaterials act as cargos loaded with reporter molecules).

### 4.1 Nanocatalysts

Catalytic signal amplification has become an essential tool in biology, where methods such as ELISA incorporating

colorimetric, fluorescent or electrochemical detection are well-established.<sup>52</sup> Despite their high activity and specificity, enzyme-based assays suffer from a number of intrinsic limitations, such as poor stability, high production costs, and difficulties associated with storage. All of these prevent them from applications in harsh or remote environments.<sup>53</sup> Nanomaterials have emerged as an attractive alternative to enzyme-based assays, not only due to their enzyme-mimicking characteristics (which gives rise to the term ‘nanozymes’<sup>54</sup>) but also due to their multi-functionality. In a seminal report, Gao *et al.* reported the use of magnetic  $\text{Fe}_3\text{O}_4$  nanoparticles as peroxidase-mimicking nanomaterials and demonstrated their multifunctional nature. In such a system, nanoparticles are able to capture target analytes, extract them from the sample matrix and amplify the signal for the colorimetric immunoassay.<sup>55</sup> In other words, nanomaterials are able to carry a large amount of recognition elements, such as antibodies, ssDNA or aptamers, but still preserve their active surface. In this regard, surface engineering of nanomaterials plays a key role in the optimization of biosensor performance, balancing the trade-off between capturing and catalytic capabilities.<sup>56</sup> In an optimized assay, nanocatalysts decorated with antibodies can lose up to 50% of their activity compared to their ‘naked’ counterparts in conditions yielding maximal signal intensity.<sup>57</sup> Accordingly, catalytic performance will be determined by a number of parameters, including composition, doping, size, surface coverage, experimental conditions, sample type, and detection methods.

Electrocatalytic amplification for microRNA detection was reported in 2006 by Gao and co-workers, using  $\text{OsO}_2$  nanoparticles to catalyze the decomposition of hydrazine.<sup>58</sup> Here, an indium tin oxide (ITO) electrode, inactive to hydrazine at low potentials, was used to re-oxidize the catalyst, which enabled a detection limit of 80 fM for the extraction of RNA in a buffer solution, with a 60 minute hybridization step.<sup>58</sup> This electrochemical signal can be

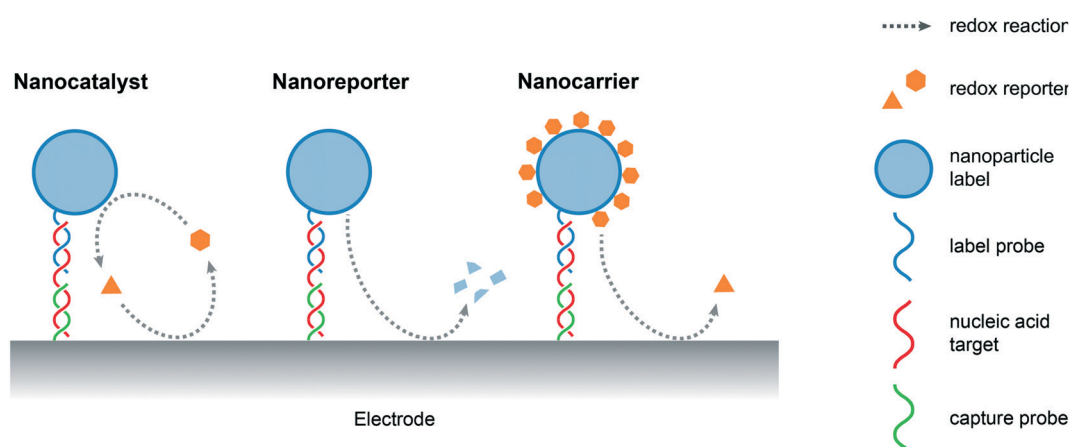


Fig. 2 Schematic overview of the role of nanomaterials in electrochemical signal amplification (based on a simplified sandwich assay) for the detection of nucleic acids. Nanomaterials can act as (i) nanocatalysts that promote the generation of electrochemically active species, (ii) redox-active nanoreporters and (iii) nanocarriers loaded with redox reporter molecules.



further amplified by designing a redox cycling system.<sup>59</sup> In such a method, a reversible redox probe with a fast kinetic response, produces a detectable signal at the working electrode that is regenerated by a catalyst (chemical-electrochemical redox cycling)<sup>60</sup> or by the counter electrode in a microsystem (electrochemical-electrochemical redox cycling),<sup>52</sup> effectively forming a cyclic reaction pathway. It should be noted that in order to achieve ultrasensitive detection, redox-cycling systems should be designed to have faster kinetics than any side reactions.<sup>59</sup> Design requires careful consideration of the electroactive species involved and the types of electron transfer involved.<sup>61</sup>

Progress in enzyme-mimicking nanomaterials has been extensively discussed in an excellent recent review.<sup>56</sup> In electrochemical systems, an emerging strategy is to employ composite nanomaterials to improve catalytic performance or add new functionalities.  $\text{Fe}_3\text{O}_4$  nanoparticles were amongst the first nanocatalysts used for signal amplification in a biological assay,<sup>62</sup> due to their ferromagnetic properties that greatly facilitate sample preconcentration and washing steps. Their multifunctional nature has facilitated new strategies in electrochemical biosensing. For example, Yadav *et al.* developed a composite nanomaterial comprising  $\text{Fe}_3\text{O}_4$  core particles decorated with Au nanoclusters that functionalize the particle with nucleic acids *via* gold-RNA interactions.<sup>63</sup> In follow-up studies, the authors further presented a complete assay for miRNA detection from cell culture and patient samples.<sup>64,65</sup> As illustrated in Fig. 3, miRNA is purified and extracted from the sample using commercial magnetic particles. This is followed by the conjugation and immobilization of the target on the electrode using the

$\text{Fe}_3\text{O}_4@\text{Au}$  nanoparticles. Subsequently, ruthenium-based redox reporter molecules can be detected by chronocoulometry. In addition, results demonstrated an improvement in the limit of detection (LOD) of three orders of magnitude (to 100 aM) when using ferrocyanide as the reducing agent.<sup>64,65</sup> That said, the exact contribution of the nanoparticles to the catalytic cycles with the reducing agent remains unclear. Overall, the method leads to a time-to-result of approximately 2 hours and highlights the importance and challenges associated with the development of a full diagnostic assay from sample collection to result. Finally, other approaches have been proposed to increase the activity of the catalytic cycle using the synergetic effects of  $\text{Fe}_3\text{O}_4$  nanoparticles bound to metal complexes, such as Cu(II)-based organometals.<sup>66</sup>

Catalytically active nanoparticles benefit from a support material that maximizes the number of catalytic sites, whilst minimizing the amount of material used.<sup>67</sup> A number of systems have been recently reported in the literature for miRNA and DNA detection using supported catalysts for signal amplification, such as Pt nanoparticles supported by  $\text{TiO}_2$  nanospheres,<sup>68</sup> Pt or Pd nanoparticles supported by metal-organic frameworks (MOFs),<sup>69,70</sup> Pt nanoparticles supported by graphene,<sup>71</sup> fullerene- $\text{CeO}_2$  composites with Pt nanoparticles<sup>72</sup> and  $\text{Fe}_3\text{O}_4/\text{CeO}_2$  composites decorated with Au nanoparticles.<sup>73</sup> These approaches demonstrate superior performance when compared to associated bare catalyst nanoparticle systems, owing to the increase of active surface area and synergetic interactions with the support materials. Nevertheless, composite nanomaterial platforms often demand multiple synthetic steps, which limit their

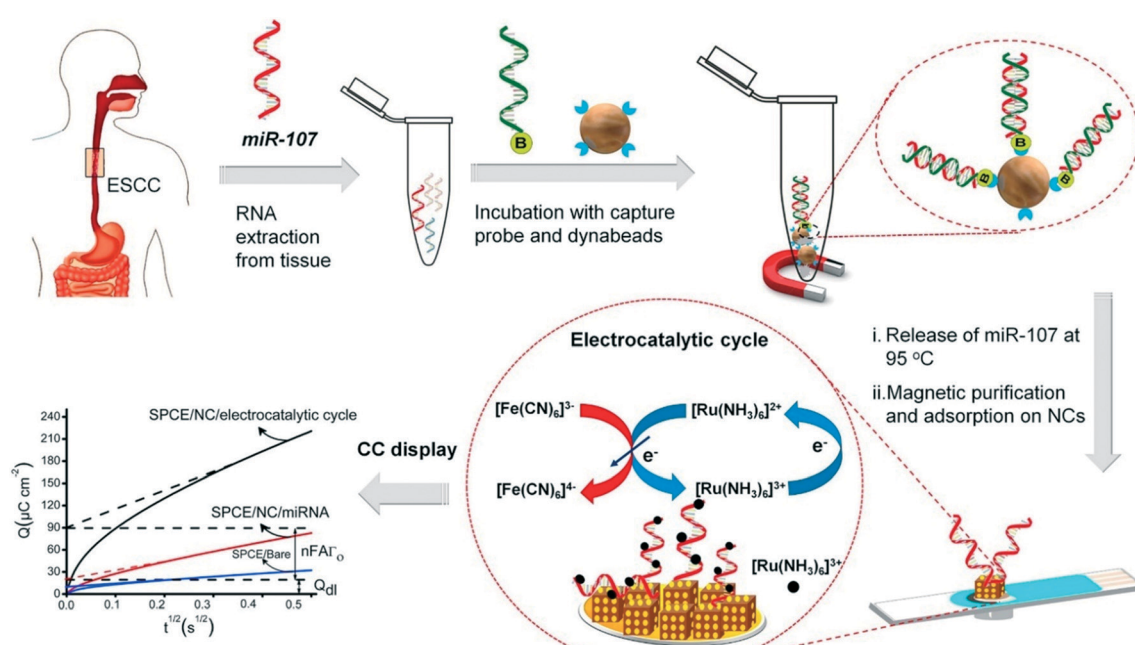


Fig. 3 Multifunctional capabilities of iron oxide nanoparticles in electrochemical biosensing, include analyte capture and sample preconcentration and electrocatalysis for signal amplification. Images reproduced with permission from ref. 65. Copyright © (2018) Elsevier.



scalability. Accordingly, MOFs (metal organic frameworks), which can be synthesized in a single step, have been suggested as a promising electrocatalyst for biosensing.<sup>74</sup> The metal centers afford catalytic activity to the MOF nanomaterials, with the surface open to functionalization with biomolecules *via* organic ligands. There have been several reports demonstrating the peroxidase-mimicking properties of MOFs functionalized with streptavidin for DNA detection, either as an indirect label that binds to a streptavidin aptamer when target DNA is absent,<sup>75</sup> or as a direct label, binding the biotinylated complementary DNA strand.<sup>76,77</sup> Recent advances in catalysis and magnetic separation of MOFs, suggest that such materials hold significant promise for electrochemical signal amplification.<sup>78,79</sup>

Sandwich type assays, where the target is immobilized between a capture and label probe, represent the most common approach for nanoparticle-based nucleic acid sensors. Taking advantage of direct interactions between nanomaterials and nucleic acids, the affinity reaction of the label may be bypassed. For example, carbon nitride nanosheets have been used as indirect labels in biosensing due to their strong interactions with ssDNA *via*  $\pi$ - $\pi$  interactions. When no target NA strands are present, nanosheets bind the unhybridized capture NA probes and subsequently catalyze the oxidation of  $\text{H}_2\text{O}_2$ , thereby generating an electrochemical response.<sup>80</sup> Alternatively, certain metals ions, such as  $\text{Ag}^+$ ,<sup>81</sup>  $\text{Cu}^{2+}$ ,<sup>82</sup> or  $\text{Pd}^{2+}$ ,<sup>83</sup> interact with dsDNA and can be metallized *in situ* to form electrocatalytically active nanoclusters, which will be discussed in detail later. The non-specific labelling the NA targets implies that the detection of nucleic acids does not discriminate based on NA sequence, but can be achieved without the hybridization step. In other words, a fully non-

specific approach does not result in a stand-alone diagnostic assay but serves as a test to detect the presence of nucleic acids within a sample. In this regard, Kim *et al.* reported a sensor based on  $\text{CeO}_2$  nanoparticles for the detection of PCR products.<sup>84</sup> The catalytic activity of  $\text{CeO}_2$  nanoparticles was found to be inhibited when dsDNA amplicons are adsorbed on the surface, as shown in Fig. 4.<sup>84</sup> Such an electrochemical amplification and detection required only 6 minutes, with a proof-of-concept assay being applied to clinical samples. In this case, for the detection of amplified products, an ultralow detection limit is not necessary as the sensors should return a negative response when measuring unamplified DNA. Nevertheless, the assay remained prone to interfering agents present in human serum (due to the non-specific nature of the detection) and exposed the assay to a large number of false positives.

Due to their rapid and quantitative nature, one can also incorporate electrochemical biosensors with other established nucleic acid amplification strategies. For example, the Merkoçi group reported an assay for the *Leishmania* DNA detection from blood samples using isothermal amplification with modified primers and electrochemical detection.<sup>85</sup> The reverse primer was labelled with a magnetic bead for facile purification and immobilization of the amplicon on the electrode, and the forward primer was bound to a gold nanoparticle to amplify the signal by catalysing the hydrogen evolution reaction (Fig. 5). Importantly, the entire procedure required less than 20 minutes at a constant temperature of 37 °C, with a detection limit of approximately one parasite per milliliter of

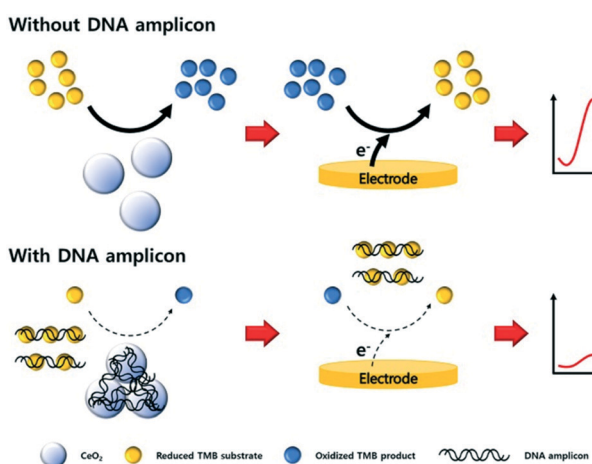


**Fig. 4** Non-specific detection of PCR products with cerium oxide nanoparticles. The adsorption of amplicons on the surface of the particles block the electrocatalytic activity of the material, thus diminishing the biosensor response proportionally to the concentration of PCR products. Images reproduced with permission from ref. 84. Copyright © (2019) Elsevier.

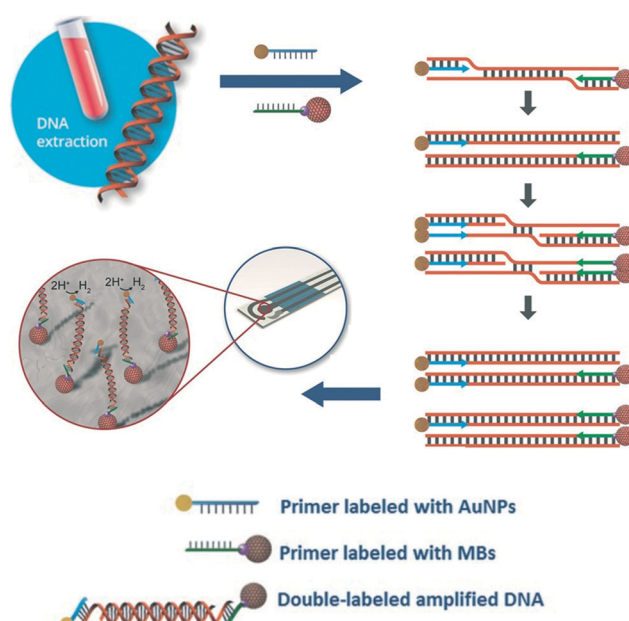


**Fig. 5** Incorporation of nanoparticles with isothermal nucleic acid amplification. The forward and reverse primers are modified with gold and iron oxide nanoparticles, respectively, enabling simple sample pre-concentration and signal amplification. Images adapted with permission from ref. 85. Copyright © (2016) John Wiley and Sons.



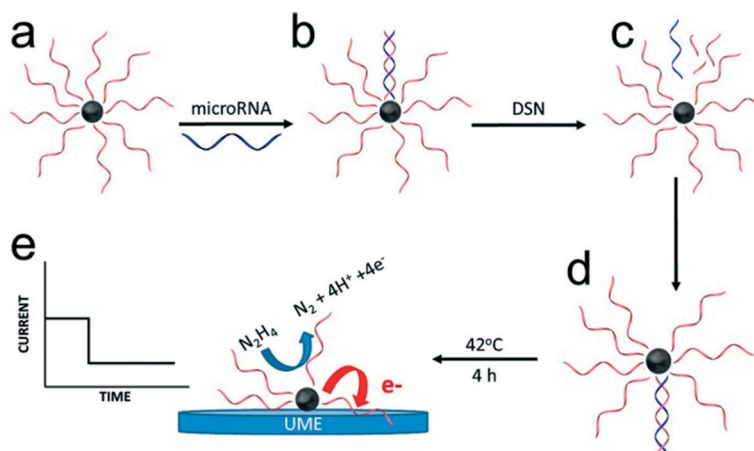


**Fig. 6** Electrocatalysis of freely diffusing platinum nanoparticles. An enzyme-assisted target recycling mechanism exposes the catalytically-active nanoparticle surface in the presence of target miRNAs, and is followed by the addition of hydrazine. The electrochemical signal generated by the catalytic decomposition of hydrazine is proportional to the exposed surface of Pt nanoparticles. Images reproduced with permission from ref. 86. Copyright © (2017) American Chemical Society.

blood, offering a promising approach for point-of-care testing on clinical sample with minimal sample pretreatment.

In most of the approaches discussed so far, the target DNA and nanoparticle labels are immobilized on the electrode surface. Conversely, Crooks and co-workers have described a fundamentally different approach, where platinum nanocatalysts freely diffused in solution and generate a detectable signal on colliding with the electrode surface (Fig. 6).<sup>86</sup> Specifically, nanoparticles were initially functionalized with ssDNA complementary to the target microRNA. This was followed by incubation with the target probe and a nuclease enzyme. Subsequently, cleavage of the hybridized probes exposes the catalytically-active nanoparticle surface, which in turn activates target recycling. Finally, the particle/DNA complexes were incubated in hydrazine, so that an electrochemical signal was generated from the catalyzed hydrazine decomposition reaction as a result of particle collisions with the gold ultra-microelectrode. The merit of this approach lies in its simplicity and versatility when compared to other methods. However, to date it has only been reported in buffer (and not complex biological media) and concentration detection limits are relatively high ( $\sim 5$  pM).

In electrocatalysis, amperometry and voltammetry are the primary electrochemical detection methods used to quantify electroactive species produced by catalytic amplification. Alternatively, electrochemical impedance spectroscopy (EIS), one of the most well-established electrochemical methods, has also been leveraged to measure the extent of electrocatalytic reactions *via* the determination of the charge transfer resistance.<sup>87</sup> For example, Peng *et al.* developed a hybridization-based miRNA biosensor using RuO<sub>2</sub> nanoparticle labels to catalyze the polymerization of 3,3-dimethoxybenzidine (DB). This reaction produces an insulating layer of poly-DB on the electrode that alters the impedance response.<sup>88</sup> That said, the polymerization reaction has to be run for at least an hour before detection by EIS. In conclusion, electrocatalysis offers

excellent performance with respect to signal amplification, especially when combined with redox cycling. However, careful consideration of nanomaterial surface engineering is required to ensure optimal performance.

#### 4.2 Nanoreporters

In regard to the use of electroactive nanomaterials as reporters in biosensor applications, we now discuss redox-active nanomaterials, particularly those containing transition metals, which can be detected electrochemically. It should be noted that electrochemical signals scale with the number of detected atoms or ions, and thus are proportional to the volume of reporter. A simple approach, for example, involves labelling the target nucleic acid with a single nanoparticle. In this regard, Crooks and co-workers reported a method for the detection of hepatitis B DNA by hybridizing the target probe between a magnetic bead and a silver nanoparticle (AgNP).<sup>89</sup> After hybridization and magnetic extraction, AgNPs were mixed with an oxidizing agent, to allow the detection of silver ions by anodic stripping voltammetry. Significantly, the authors reported a 250 000-fold signal amplification using 20 nm AgNPs (when compared to methylene blue-labelled DNA) and a concentration detection limit of 85 pM on a paper-based device containing screen-printed electrodes. The ability to perform signal amplification within a paper device demonstrates the strength and simplicity of the approach, with only mild reagents and short incubation time being used. Several methods have also been used to further amplify signal, primarily by increasing the number of AgNPs per target strand. For example, a rolling circle amplification step was implemented followed by hybridization of AgNPs periodically along the elongated DNA strand (Fig. 7).<sup>90</sup> Alternatively, the use of a support material,<sup>91</sup> dendritic AgNPs,<sup>92</sup> and AgNPs covalent aggregates<sup>93</sup> have also examined.

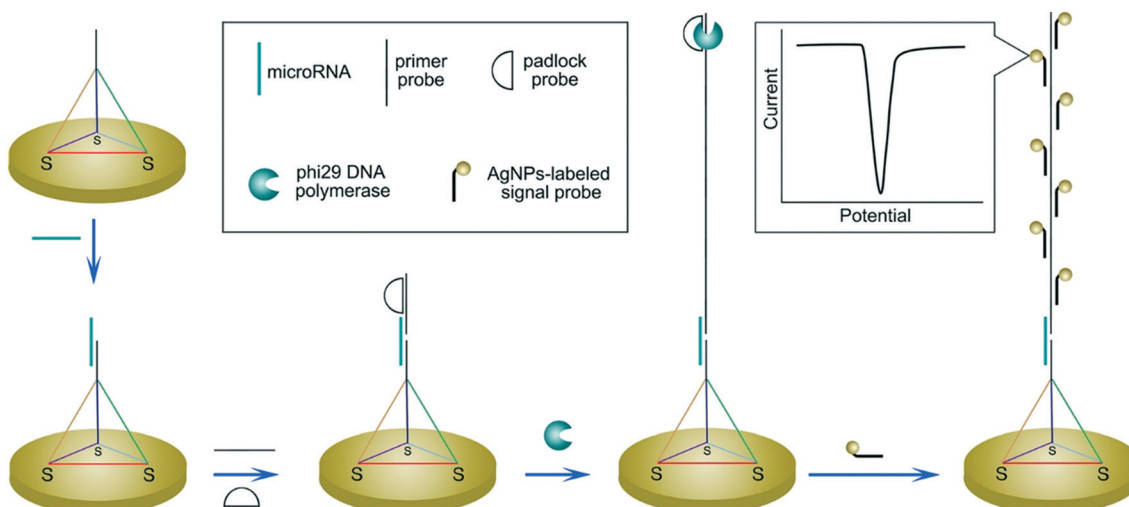


**Fig. 7** Increasing the number of binding sites for electroactive reporters *via* nucleic acid elongation. Rolling circle amplification creates periodical hybridization binding sites for DNA-labelled silver nanoparticles along the elongated strand. The increased number of silver nanoparticle labels are subsequently detected by stripping voltammetry. Images reproduced with permission from ref. 90. Copyright © (2015) American Chemical Society.

To amplify electrochemical signals without hybridizing nanoparticles labels to the target strand, *in situ* metallization of metal nanoclusters on nucleic acid strands has been demonstrated. For example, experimental studies have demonstrated the interaction of silver(I) ions with cytosine-cytosine (C–C) base pairs<sup>94</sup> and copper(II) ions with dsDNA.<sup>95</sup> Here, a typical assay involves the capture of target NAs on the electrode, which is then contacted with a solution containing metal ions to form metal nanoclusters on the nucleic acid strands, either through redox reactions with a reducing agent or *via* electrochemical/catalytic pathways.<sup>96–100</sup> Subsequently, the metal nanoclusters are dissolved using a strong acid (e.g. for Cu nanoclusters) or electrochemically (e.g. for Ag nanoclusters), and quantified by stripping voltammetry.<sup>96,97</sup> Recent studies have also reported the combination of metallization and hybridization chain reaction (HCR) to increase the number of binding sites for metal ions. Elongation probes are designed to form C-rich loops as seed sites for Ag nanoclusters,<sup>98</sup> or Y-shaped dsDNA shapes for Cu nanoclusters.<sup>99</sup> Gold nanoparticles have also been decorated with C-rich DNA strands to offer an increased number of seed sites for silver metallization.<sup>101</sup> Alternatively, graphene oxides can be used as a catalytic platform to assist in the *in situ* formation of Ag or Prussian blue nanoparticles.<sup>102,103</sup> Here, graphene oxide interacts with the unhybridized capture ssDNA *via*  $\pi$ - $\pi$  interactions and amplifies the signal when no target analytes are present in the sample, *i.e.* a ‘signal-off’ sensor.<sup>102,103</sup>

Direct detection of the nanoparticle labels also offers the possibility of multiplexing signals by incorporating nanomaterials with distinguishable redox peaks. For example, Merkoçi *et al.* have pioneered the use of quantum dots for multiplexed electrochemical biosensing.<sup>104</sup> This approach enabled the simultaneous detection of three DNA targets with PbS, ZnS and CdS quantum dot (QD) labels, with

detection limits down to 270 pM for single QD labels and 2.7 pM for QDs loaded on latex beads. Building on this approach, recent advances include the integration of QDs labels with other amplification methods, such as nucleic acid amplification,<sup>105</sup> target recycling<sup>106</sup> or DNA elongation to increase the number of labels per target.<sup>107</sup> Despite the excellent detection limits, down to femtomolar levels, the use of toxic heavy metals and the requirement of time-consuming dissolution steps remain a concern.<sup>105,106</sup>

#### 4.3 Nanocarriers

Nanomaterials acting as cargos for redox reporters represent one of the most straightforward approaches for electrochemical signal amplification and have been widely used for nucleic acid detection. As one of the first strategies for amplifying biosensing signals, nanocarrier methods have seen relatively limited development in the past five years. That said, Kaur *et al.* reported a DNA biosensor based on a cobalt-porphyrin redox marker.<sup>108</sup> They observed a 1000-fold enhancement in the detection limit (3.8 aM) of short DNA sequences in buffer when loading the organometallic compounds on gold nanoparticles.<sup>108,109</sup> A variety of nanoparticle-marker systems have been reported in recent years, including gold nanoparticles with methylene blue<sup>110</sup> or ferrocene,<sup>111</sup>  $\text{Fe}_3\text{O}_4$  nanoparticles with thionine or ferrocene,<sup>112</sup> multi-walled carbon nanotubes with thionine,<sup>113</sup> polymer nanoparticles with  $\text{Cu}^{2+}$  ions,<sup>114</sup> and titanium phosphate nanoparticles with  $\text{Cd}^{2+}$  ions.<sup>49</sup> More recently, versatile nanoporous MOFs have demonstrated high loading capacities for a variety of redox reporters, including ions (e.g.  $\text{Cd}^{2+}$ ,  $\text{Pb}^{2+}$ ),<sup>115</sup> organometals (e.g. ferrocene),<sup>116</sup> and small molecules (e.g. methylene blue, 3,3',5,5'-tetramethylbenzidine).<sup>116,117</sup>

Interactions between redox markers and nanoparticles include covalent bonds,<sup>112,113</sup> electrostatic interactions,<sup>49</sup>



nano pore intercalation,<sup>114,115</sup> physisorption,<sup>116,117</sup> and gold-thiol interactions,<sup>110,111</sup> which control the loading process. The ability to load nanoparticle labels with several signal probes, such as Cd<sup>2+</sup>/Pb<sup>2+</sup> or methylene blue/ferrocene, enables a ratiometric signal analysis, using a dual-probe system to detect the ratio of the probe signal with respect to a reference. By using a ferrocene labelled hairpin probe on an electrode surface, and methylene blue on the nanoparticle tag, detection of the target analyte is more robust, since non-specific adsorptions events of the nanoparticle labels on the electrode can be accounted for from the signal ratio.<sup>110</sup>

More generally, recent research efforts have been focused on surface engineering of nanoparticle labels, with a view to increasing the loading capacity of redox indicators. For example, one can functionalize gold nanoparticles with dsDNA or ssDNA to increase the number of possible binding sites for RuHex<sup>118</sup> or methylene blue labels,<sup>119</sup> respectively. Alternatively, gold nanoparticles can form hybridization-induced aggregates upon target recognition, which offer more binding sites for RuHex. In this manner, a 32-fold enhancement in detection limits has been reported when compared to a single gold nanoparticle label.<sup>120,121</sup>

On the other hand, a unique approach for miRNA detection was recently described by Gooding and co-workers, as illustrated in Fig. 8.<sup>122</sup> Here, gold-coated magnetic nanoparticles were conjugated with complementary ssDNA labelled with methylene blue, and mixed with the sample solution containing target miRNAs. Nanoparticles were then brought in contact with the electrode using a magnetic field, generating a superlattice whose structure depends on the presence of dsDNA, and thus indicative of hybridized targets. Gold nanoparticles acted as the electrode material and the recorded signal was minimized as the presence of rigid hybridized probes (dsDNA) diminishes structural compactness. In this instance, the nanoparticles serve a dual purpose, not only acting as a nanocarrier for redox reporters, but also improving charge transport properties and thus

signal transduction. It was found that the method enables the detection of targets down to 10 aM in whole blood, with a remarkably broad linear range of over 7 orders of magnitude. The use of magnetic core-shell nanoparticles enables the extraction of target miRNAs from blood samples after a 30 minute hybridization step, followed by a 5 minute step for electrochemical quantification.

#### 4.4 Materials considerations

Table 1 summarizes the aforementioned roles of nanomaterials for amplifying electrochemical signals. The limits of detection and sample matrices are also indicated. We now discuss the application of noble metals,<sup>123</sup> metal oxides,<sup>124</sup> quantum dots,<sup>125</sup> 2D nanomaterials, and MOFs<sup>126</sup> for electrochemical signal amplification.

**Noble metals.** Noble metals are among the most commonly used nanomaterials in electrochemistry due to well-established synthetic protocols, high conductivity and an in-depth understanding of their fundamental properties.<sup>127</sup> In particular, gold nanoparticles have demonstrated excellent potential as cargos for redox markers, taking advantage of the strong interactions between gold and thiolated nucleic acids.<sup>108,109</sup> The prospect of gold nanoparticles in signal amplification, nevertheless, remains unclear, because they exhibit broad redox peaks, as a consequence of their multivalences, as well as a low electrocatalytic activity.<sup>128</sup> On the other hand, silver ions exhibit exceptional sensitivity for electrochemical detection and generate sharp redox peaks.<sup>129</sup> Silver nanoparticles can be used as labels or formed *in situ* by metallization.<sup>94</sup> The ability to form silver nanoclusters *in situ* without requiring a label NA strand and high analytical sensitivity make this one of the most promising signal amplification methods for biosensing.<sup>45</sup> Similarly, copper nanoclusters can also label captured NA strands *via* metallization, showing greater stability than silver, but exhibiting broader redox peaks, due to the underlying two-

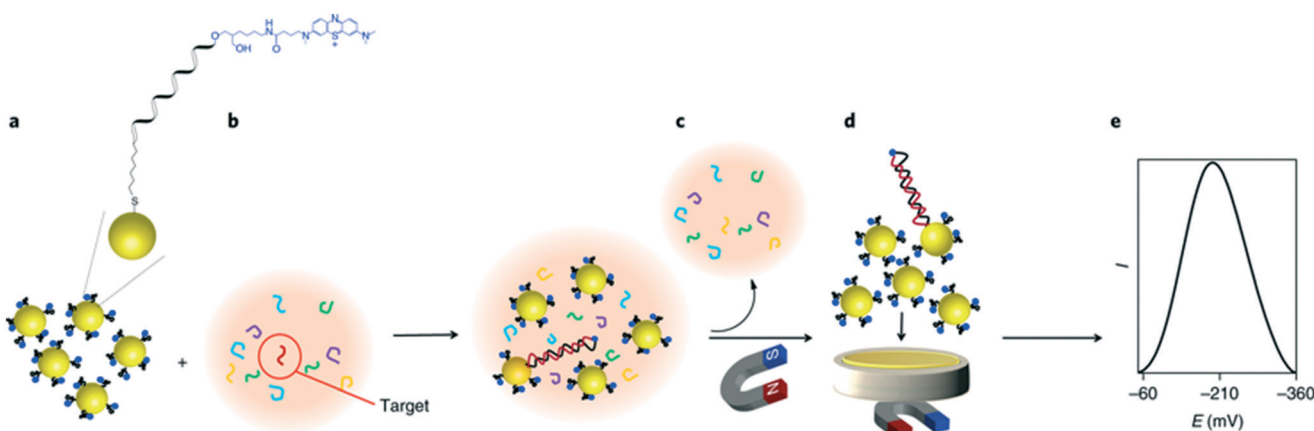


**Fig. 8** Gold nanoparticle networks as a DNA sensitive electrode. Iron oxide core/gold shell nanoparticles, functionalized with redox labelled single stranded DNA form a compact superlattice on the electrode when a magnetic field is applied. The compactness of this network is sensitive to the presence of hybridized double stranded DNA on the particle surface, therefore strongly impacting the electrochemical signal when a target sequence is present in the sample. Images reproduced with permission from ref. 122. Copyright © (2018) Springer Nature.



**Table 1** Summary of selected nanomaterials recently reported for electrochemical signal amplification for the detection of nucleic acid targets. Composite nanomaterials are sorted according to the core material, with the core@shell or support@surface species notation being used

Type	Nanomaterials	Signal amplification strategy	Redox indicator	Nucleic acid amplification	Sample	LOD	Ref.	
Noble metals	Au NPs	Nanocatalyst	Hydrogen evolution	RPA	Blood	~20 aM	85	
	Au NPs	Nanocarrier	Co(II) porphyrin	—	Buffer	3.8 aM	108	
	Au NPs	Nanocarrier	Ferrocene	—	Buffer	0.37 fM	111	
	Au NPs	Nanocarrier	RuHex	—	Buffer	1.0 fM	118	
	Au NPs	Nanocarrier	RuHex	EATR + CHA	Buffer	25 aM	120	
	Au NPs	Nanocarrier	RuHex	HCR	Serum	0.12 fM	121	
	Au NPs	Nanocarrier	Methylene blue	—	Blood	10 aM	122	
	Ag NPs	Nanoreporter	Ag <sup>+</sup>	—	Buffer	85 pM	89	
	Ag NPs	Nanoreporter	Ag <sup>+</sup>	RCA	Serum	50 aM	90	
	Ag NP dendrimers	Nanoreporter	Ag <sup>+</sup>	—	Buffer	0.78 pM	92	
	Ag NP aggregates	Nanoreporter	Ag <sup>+</sup>	—	Serum	20 aM	93	
	Metallized Ag nanoclusters	Nanoreporter	Ag <sup>+</sup>	EATR + HCR	Serum	0.64 fM	98	
	Metallized Ag nanoclusters	Nanoreporter	Ag <sup>+</sup>	—	Buffer	0.16 fM	101	
	Metallized Cu nanoclusters	Nanoreporter	Cu <sup>2+</sup>	EATR + HCR	Serum	10 aM	99	
	Metallized Cu nanoclusters	Nanoreporter	Cu <sup>2+</sup>	EATR + HCR	Cell lysate	45 aM	96	
	Pt NPs	Nanocatalyst	Hydrazine	—	Buffer	45 pM	86	
	Fe <sub>3</sub> O <sub>4</sub> @Au NPs	Nanocatalyst	RuHex	—	Cell lysate	100 fM	64	
Metal oxides	Fe <sub>3</sub> O <sub>4</sub> NPs @ Cu(II) thiosemicarbazide	Nanocatalyst	TMB	HCR	Serum	33 aM	66	
	Fe <sub>3</sub> O <sub>4</sub> NPs	Nanocarrier	Thionine/ferrocene	HCR	Cell lysate	0.28 fM	112	
	CeO <sub>2</sub> NPs	Nanocatalyst	TMB	PCR	Serum	33 aM	84	
	CeO <sub>2</sub> @Pt NPs	Nanocatalyst	H <sub>2</sub> O <sub>2</sub>	—	Serum	0.33 fM	72	
	CeO <sub>2</sub> /Fe <sub>3</sub> O <sub>4</sub> @Au NPs	Nanocatalyst	Methylene blue	CHA	Serum	0.33 fM	73	
	PbS and CdS NPs	Nanoreporter	Pb <sup>2+</sup> and Cd <sup>2+</sup>	—	Serum	12 fM	105	
	CdS NPs	Nanoreporter	Cd <sup>2+</sup>	EATR	Cell lysate	0.48 fM	106	
	Carbon-based nanomaterials	Graphene@Ag NPs	Nanocatalyst/ nanoreporter	Ag <sup>+</sup>	EATR	Buffer	57 aM	71
	Graphene oxide@Ag NPs	Nanocatalyst/ nanoreporter	Ag <sup>+</sup>	—	Serum	7.6 fM	102	
	Graphene oxide@Prussian blue	Nanocatalyst/ nanoreporter	Prussian blue	—	Serum	1.5 fM	103	
MOFs	Multiwalled carbon nanotubes	Nanocarrier	Thionine	—	Buffer	32 fM	113	
	MOF@Pt NPs	Nanocatalyst	H <sub>2</sub> O <sub>2</sub>	—	Serum	33 aM	134	
	MOF@Pd NPs	Nanocatalyst	NaBH <sub>4</sub>	—	Buffer	33.6 fM	69	
	MOF@Fe(III) porphyrin	Nanocatalyst	o-Phenylenediamine	—	Serum	0.48 fM	75	
	MOF@Fe(III) porphyrin	Nanocatalyst	H <sub>2</sub> O <sub>2</sub>	—	Buffer	0.69 fM	76	
	Zr(IV)-MOF	Nanocatalyst	O <sub>2</sub>	EATR	Serum	0.29 fM	77	

Abbreviations: CHA: catalytic hairpin assembly, EATR: enzyme-assisted target recycling, HCR: hybridization chain reaction, LOD: limit of detection, MOF: metal–organic framework, NP: nanoparticle, PCR: polymerase chain reaction, RCA: rolling circle amplification, RPA: recombinase polymerase reaction, RuHex: hexaaminoruthenium(III), TMB: 3,3',5,5'-tetramethylbenzidine.

electron process.<sup>44</sup> Silver and copper can also act as electrocatalysts for the reduction of H<sub>2</sub>O<sub>2</sub>, in spite of their limited activity.<sup>81,82</sup> Lastly, platinum nanoparticles have demonstrated the highest activity amongst peroxidase-mimicking materials and possess a high compatibility with a wide range of substrates, thereby also giving excellent electrocatalytic amplification.<sup>68,71,72</sup>

**Metal oxides.** The catalytic properties of Fe<sub>3</sub>O<sub>4</sub> have been known for more than a decade, and the material has been widely adopted for electrochemical amplification purposes.<sup>55</sup> Due to its multifunctional nature, Fe<sub>3</sub>O<sub>4</sub> has found numerous applications for signal amplification; as electrocatalysts, as a support material for redox indicators or as part of composite

nanomaterials.<sup>130</sup> Additionally, their ferromagnetic properties greatly facilitate the pre-concentration of target analytes from complex samples and their subsequent immobilization on the electrode.<sup>85</sup> Cerium oxide has also attracted attention as a support material (e.g. for Pt nanoparticles) or as electrocatalysts.<sup>72,73,84</sup> Its catalytic properties are tunable and strongly depend on the concentration of oxygen vacancies on the surface, which can be controlled during synthesis.<sup>131</sup> However, metal oxide nanoparticles are often synthesized using solvothermal methods at elevated temperatures, and thus difficult to biofunctionalize.<sup>124</sup>

**Quantum dots.** Based on the success of metal chalcogenide quantum dots, such as ZnS, CdS, PbS, as



fluorescent labels for biosensing, they have also been examined as labels for electrochemical detection.<sup>125</sup> Indeed, the sharp and distinguishable redox peaks of the metal ions have been shown to allow for multiplexed detection of up to three analytes with only one sensor.<sup>104</sup>

**2D materials.** Two-dimensional (2D) nanomaterials have been widely applied for electrode modification, leading to remarkable improvements in signal transduction<sup>132</sup> and tunability of surface properties.<sup>133</sup> For signal amplification, 2D nanosheets have been used as high surface area cargos for redox markers, such as graphene and graphene oxide, and catalysts, such as carbon nitride for redox cycling and metallization.<sup>71,80,102,103</sup>

**Metal organic frameworks.** MOFs have been considered as one the most versatile platforms for signal amplification.<sup>126</sup> The high number of combinations of organic ligands and metal centers provide a route to tuning signal amplification characteristics, enabling loading of redox markers in nanopores, direct detection of electroactive metal centers and electrocatalysis. Nevertheless, further development of MOF nanomaterials for biosensing applications will be required, specifically in regard to their stability.<sup>126</sup>

In conclusion, signal amplification using nanomaterials as cargos has evolved from commonly used single redox marker labels, and provides for an increased number of redox reporters at the electrode. The loading capacity of nanoparticle labels however limits amplification potential. The use of nanomaterials as redox reporters is simple to implement, provides for amplification factors of five to six orders of magnitude and can be easily combined with *in situ* metallization. That said, performance highly depends on the choice of nanoparticle label, and the general method requires an additional step to convert the nanomaterial to a detectable form. Finally, electrocatalysis represents one of the most powerful amplification tool in electrochemical biosensing and strongly benefit from the high catalytic activity and multifunctional nature of nanomaterials. However, the approach requires an additional incubation period with the substrate solution and does not currently allow multiplexed analysis.

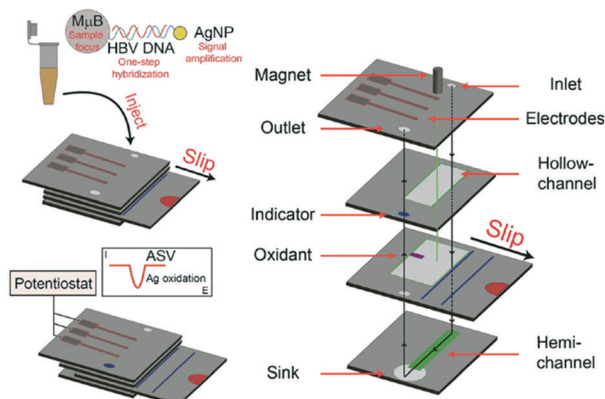
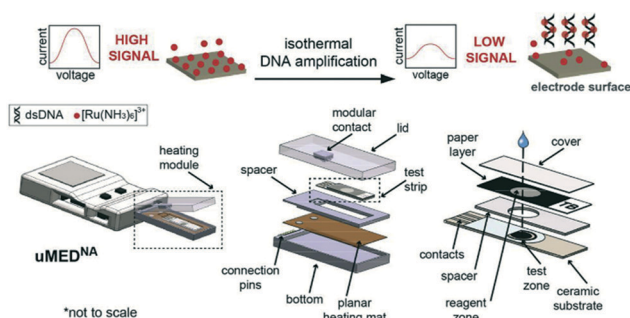
## 5. Applications for point-of-care diagnostics

In 2003, the World Health Organization (WHO) introduced the 'ASSURED' criterion to define the ideal features of point-of-care (POC) diagnostic tests.<sup>39</sup> Put simply, such tests should be affordable, sensitive, specific, user-friendly, rapid and robust, equipment-free and deliverable to end-users.<sup>39</sup> Recently, Peeling and colleagues<sup>135</sup> suggested two additions to these basic requirements. Real-time connectivity for digital healthcare<sup>136</sup> and ease of sample collection yield the 'REASSURED' criterion.<sup>135</sup> Indeed, sample collection and pretreatment remain a major challenge hindering the translation of biosensing strategies from laboratory settings to the field. To address this wish list, analytical

instrumentation can be miniaturized and made to handle ultra-small sample volumes with minimal user input using the principles of microfluidics.<sup>137–139</sup> Such microscale systems can be easily integrated with external electronic architecture, to enable the performance of multistep assays with minimal user input.<sup>140</sup> In particular, microfluidic paper-based analytical devices ( $\mu$ PADs) offer an ultra-low cost platform to perform assays. Here, capillary flow is driven by the wicking properties of paper, owing to its microporous and hydrophilic structure, and thus pumps or other fluid actuation systems are not required.<sup>141</sup>  $\mu$ PADs have been extensively applied for the detection of infectious diseases, with several diagnostic tests being approved by the WHO for the detection of malaria and HIV at the POC.<sup>141,142</sup> However, colorimetric readout only provides for a semi-quantitative interpretation of the result, with bulky and expensive instrumentation normally being needed for quantification. To address this need, Henry and co-workers pioneered electrochemical detection in  $\mu$ PADs, using screen-printed electrodes for the rapid and quantitative determination of analyte concentrations.<sup>143</sup> Since this seminal work, a wide range of techniques have been developed to fabricate and pattern electrodes on  $\mu$ PADs; including screen printing and inkjet printing of conductive inks,<sup>144</sup> evaporation or sputtering of metals,<sup>145</sup> as well as "reagentless" techniques such as laser scribing.<sup>146</sup>

Very recently, exciting advances have been made in relation to the detection of nucleic acids on  $\mu$ PADs. For example, Crooks and co-workers presented an origami-inspired device comprising multiple sliding layers of paper that allowed for electrochemical detection of short target DNA sequences.<sup>147</sup> In a subsequent study, the authors implemented a signal amplification strategy (using silver nanoparticles) for the detection of the hepatitis B virus at picomolar concentrations (see Fig. 9A).<sup>148</sup> Briefly, the hybridization of the target was first performed in a vial followed by introduction onto the  $\mu$ PAD. Subsequently, the top layer was slid to dispense pre-dried  $\text{KMnO}_4$ , with silver ion concentration being quantified by the stripping voltammetry. Alternatively, Kokkinos *et al.* more recently described a paper-based lateral flow assay with quantum dots labels using a sputtered tin working electrode, in which  $\text{CdSe/ZnS}$  core/shell nanoreporters were dissolved using  $\text{HCl}$  and  $\text{Cd}^{2+}$  ions detected by stripping voltammetry.<sup>145</sup> Furthermore, Whitesides and colleagues reported the first fully integrated and portable  $\mu$ PAD that combines nucleic acid isothermal amplification with electrochemical readout for the detection of *M. tuberculosis* genomic DNA (Fig. 9B).<sup>149</sup> Here, the paper layer is sandwiched between the screen-printed carbon electrodes and a heating element. Recombinase polymerization reaction (RPA) reagents were mixed with the target DNA and RuHex redox reporters, and loaded onto paper. The detection of amplicons by square wave voltammetry afforded a detection limit of  $11 \text{ CFU mL}^{-1}$  after a 20 minute RPA. This proof-of-concept study demonstrated a fully integrated and automated assay for



**A****B**

**Fig. 9** Integration of nucleic acid electrochemical detection in self-contained device for point-of-care application. (A) Multilayer paper-based device with screen-printed electrodes capable of performing a multi-step assay with electrochemical detection for the detection of hepatitis B virus. The sliding mechanism enables the control of the incubation and dispensing of the required reagents for the labeling of the target DNA with silver nanoparticles. Images adapted with permission from ref. 89. Copyright © (2015) American Chemical Society. (B) Fully automated and connected device for the detection of *M. tuberculosis*. The genomic DNA is amplified by isothermal amplification and detected electrochemically with limited user input. Images adapted with permission from ref. 147. Copyright © (2018) Elsevier.

pathogen detection with little demand for equipment. Although  $\mu$ PADs are ideal for simple assays, protocols requiring long incubation times and high temperatures are often compromised due to fluid vaporization. To this end, polymeric or glass microfluidic devices are better suited to fully-integrated and complex assays. For example, Plaxco *et al.* integrated a gold microelectrode and a heating block module in a polydimethylsiloxane/glass microchip to perform loop-mediated isothermal amplification (LAMP) at 65 °C over 60 minutes, and achieved a detection limit of 16 copies of *Salmonella* genomic DNA.<sup>150</sup> However, these microsystems require the use of external pumps, which hinders their use in resource-limited settings. It is clear that even though microfluidic systems greatly facilitate sample handling and integration of functional components,<sup>137</sup> they come with new challenges associated with electrochemical detection. These

include robust electrode modification and the ability to measure ultra-small currents from microelectrodes.<sup>140</sup>

Another issue relating to electrochemical biosensing is powering. Self-powered biosensors have already been demonstrated. For example, enzymatic biofuel cells at the counter electrode can provide power to the device whilst also setting the reference potential. This could be an interesting opportunity to drastically simplify device hardware.<sup>151</sup> Indeed, it is well-recognized that one of main obstacles for the implementation of electrochemical sensors, compared to colorimetric assays, at the POC is the requirement of a potentiostat.<sup>26</sup> Although portable potentiostats are now commercially available, devices with sufficient accuracy for ultrasensitive detection remain prohibitively expensive.<sup>152–154</sup> To this end, Whitesides and colleagues has developed an open-source potentiostat built using off-the-shelf components and capable of wireless communication *via* Wi-Fi or Bluetooth,<sup>155,156</sup> greatly reducing the equipment cost by more than one order of magnitude. Additionally, the connectivity of potentiostats to smartphones opens the possibility of real-time data analysis, storage and transmission of patient data, and connectivity to cloud services. With the widespread development of cellular network technologies in countries with poor access to healthcare facilities, connected diagnostic devices are expected to transform patients' access to advice and treatment.<sup>136</sup> We anticipate that the development of low-cost connected sensors will be a crucial step towards next-generation digital diagnostics for mobile health.

## 6. Outlook

### 6.1 Nanomaterial engineering challenges

As previously illustrated, nanomaterials have many advantageous features for the amplification of electrochemical signals. That said, the use of nanoparticle labels is often constrained by their high surface-to-volume ratios, which means that nanoparticles aggregate in the high ionic strength solutions commonly used for electrochemical detection. To this end, surface engineering of nanoparticles is key in generating colloidally stable nanoparticles in high saline solutions, without compromising other functions, such as the affinity of biorecognition elements, the active surface for electrocatalysis and the loading capacity of redox reporter. In addition, non-specific binding of nanoparticles to proteins and device substrates can compromise detection specificity and sensitivity, and remains one of the most common factors limiting the performance of nanoparticle-based biosensors at ultra-low concentrations. This issue can be addressed by blocking either the electrode or nanomaterial surface, but to date these approaches remain empirical and are seldom systematically optimized. Rational approaches are emerging, with progress in surface engineering of nanomaterials and fundamental interaction of materials-biomolecules interfaces.

We also note that, despite recent advances in the use of nanomaterials in electrochemical biosensing, there are no

widely-accepted benchmark method, such as gold nanoparticle labels in the case of colorimetric diagnostic tests. In this regard, there is an urgent need to establish methods that quantitatively compare novel amplification strategies. For example, the intrinsic amplification capability of a given nanoparticle label could be evaluated by directly capturing the labels on the electrode *via* biotin/avidin interaction. Put simply, standardized approaches is seldomly presented, but must be adopted to accelerate advancements in the field.

Extensive characterization of novel nanomaterials represent a crucial step for the progress of nanotechnology. In particular, electrocatalysis involves complex interfacial processes that have been examined in systems such as noble metals, metal oxides, MOFs, and carbon nanomaterials. Nevertheless, each material will catalyze a reaction *via* different mechanisms, which are poorly understood.<sup>157</sup> This issue limits the optimization and rational design of novel materials for electrocatalytic sensing. Recently, considerable efforts have been made to better characterize electrocatalytic materials, in particular with regard to stability, morphology and reaction mechanisms, using analytical tools such as mass spectrometry, electrochemical atomic force microscopy and photoelectrospectroscopy.<sup>158–160</sup>

## 6.2 Next-generation nucleic acid detection approaches

Nucleic acid detection technologies have advanced significantly in recent years. In particular, the CRISPR/Cas technologies, widely studied for their genome editing capabilities, have attracted considerable attention as a tool for nucleic acid detection.<sup>161</sup> For example, CRISPR/Cas13 and Cas12a effectors exhibit ribonuclease activity upon target recognition, enabling the detection of DNA and RNA with remarkable sensitivity.<sup>162,163</sup> This system, when combined with an isothermal amplification step, has been shown to allow detection of a single target copy per microliter of biofluid within 2 hours, using gold nanoparticle labels for colorimetric readout.<sup>162,164</sup> The assay can be adapted to other target analytes through design of an appropriate single guide RNA (sgRNA) and possesses multiplexing capabilities by combining orthogonal CRISPR/Cas systems.<sup>163</sup> Alternatively, a proof-of-concept strategy called CRISPR-Chip has described the immobilization of CRISPR/Cas9 on graphene field effect transistors (gFET) for the label-free (electrochemical) detection of unamplified DNA.<sup>165</sup> It is only a matter of time before this technology is applied to electrochemical detection with electroactive nanomaterials, representing exciting new avenues for double-signal amplification.

Next, it should be remembered that multiplexed detection of several analytes by a single biosensor remains a difficult task.<sup>166</sup> Current electrochemical strategies can detect up to three or four analytes on a single sensor; a number limited by the potential window and the intrinsic bandwidth of the redox reporter peaks.<sup>26</sup> Parallelization of biosensors detection offers a robust approach to increasing the multiplexing

capabilities of a device using standard microfabrication technologies. Systems with up to several thousand parallel electrodes have been reported for oligonucleotide detection, using enzymatic labels for signal amplification.<sup>167</sup> However, most of these approaches require bulky instrumentation or robots to pipette the reagents onto microelectrodes. Microfluidics provide a promising platform to miniaturize these highly-parallelized systems with integrated signal amplification and detection strategies.

Progress in nucleic acid sequencing is transforming both epidemiological studies and personalized medicine. Next-generation sequencing methods commonly relies on solid-state membrane materials containing nanopores, with the passage of biomolecules through the pores being detected by the a change in current.<sup>168</sup> Whilst assays based on biomarker recognition, as discussed in this review, are essentially hypothesis-driven, sequencing pathogen genomes may simultaneously yield information on the genes of interest, *e.g.* genes from well-conserved regions or those encoding antibiotic resistance, but also on mutations, creating valuable epidemiological information for disease surveillance. The commercialization and miniaturization of next-generation sequencing technology is likely to make it an interesting addition to the molecular diagnostics toolkit. Indeed, portable devices, such as the MinION by Oxford Nanopore,<sup>169</sup> are now commercially available and capable of sequencing DNAs or RNAs when simply connected *via* USB to a laptop; highlighting their potential for rapid clinical response in resource-limited settings.<sup>169</sup>

## 6.3 Alternative biomarkers

Much activity has been devoted to the search for alternative biomarkers for disease detection *via* non-invasive procedures. In particular, circulating biomarkers, such as tumour cells, miRNAs and exosomes, in body fluids has emerged as robust tools for the detection of cancers and bacterial diseases, and additionally show great promise for electrochemical detection.<sup>170–172</sup> With the ever-growing number of molecular and physiological biomarkers, precision medicine is moving towards a scenario where data analysis is carried out *via* machine learning techniques.<sup>173</sup> Indeed, the development of biosensors capable of measuring a variety of analytes will require labels and amplification methods capable of high versatility, which could in principle be fulfilled by bespoke multifunctional nanomaterials.

## 6.4 Towards decentralized healthcare

Decentralization of healthcare systems involves moving medical procedures away from hospitals and surgeries and into the home. Such a transition necessitates the development of diagnostic tests that can be reliably used at the point-of-care by untrained users. In this respect, the development of POC tests must consider not only the assay itself, but also every step between sample collection and outcome interpretation. As detection limits and sensitivities



improve, key challenges will include standardizing sensor preparation (robustness, scalability, electrode and nanomaterial synthesis), sample collection (pre-treatment and pre-concentration), assay times and quantitative performance (through positive and negative controls).<sup>174</sup> In this respect the Foundation for Innovative New Diagnostics (FIND) have compiled a list of guidelines for target product profiles, which details the minimum requirements of priority diagnostic tests to ensure that the needs of end-users are taken into account.<sup>175</sup> For example, in the detection of gonorrhoea resistance to antibiotics, an ideal test should require less than 20 minutes (excluding sample preparation), and cost less than 15 USD at volume production.<sup>175</sup> These recommendations set valuable guidelines for the development of nanomaterials-based electrochemical amplification for specific target diseases.

Ultimately, the interpretation of complex diagnostic data may always require medical specialists, with the decentralization of healthcare relying on the connection of end-users to the specialists *via* digital technology.<sup>136</sup> As such, electrochemical biosensors may become an ideal platform for mobile and digital health as they can be easily integrated with wireless communication and connected to a smartphone. With the development of mobile applications and online tools guiding patients for self-testing and follow-up, sensitive POC diagnostic tests can act as a first-round analysis before conducting more thorough laboratory tests, benefiting patients and the greater community.

## 7. Conclusion

Recent progress in nucleic acid detection offers multiple options for sensitive diagnostics with minimal equipment. Signal amplification strategies enable the development of electrochemical biosensors that access detection limits close to clinically relevant biomarker concentrations, without the need for a nucleic acid amplification step. In this review, we have attempted to highlight the multifunctional nature of nanomaterials, as electrocatalytic labels, cargos for redox indicators or reporters. Simultaneously, nanotechnology opens exciting opportunities for analyte capture and sample pre-concentration. The integration of these methods with microfluidic tools represents new pathways for the development of self-contained diagnostic tests that minimize sample handling and user input for practical clinical use. Clearly, the translation of research technologies into commercial products is an immense challenge, with few proposed methods being robust enough for commercial applications. Finally, we stress the urgent need for standard characterization procedures to understand, optimize, compare and ultimately improve the activity of nanomaterials for signal amplification.

## Conflicts of interest

There are no conflicts to declare.

## Acknowledgements

The authors would like to thank Eugenia Quach for proofreading. L. B. and C. J. S. are grateful for the financial support from the Swiss National Science Foundation (Project Number: 200021-178944). A. S. N. would like to thank the State Secretariat for Education, Research and Innovation (SERI) in Switzerland for a Swiss Government Excellence Scholarship (ESKAS No. 2016.0728).

## References

- 1 D. P. Nikolelis and G. P. Nikoleli, *Nanotechnology and biosensors*, Elsevier, 2018, vol. 22.
- 2 H. Aldewachi, T. Chalati, M. N. Woodroffe, N. Bricklebank, B. Sharrack and P. Gardiner, *Nanoscale*, 2018, **10**, 18–33.
- 3 *World malaria report*, World Health Organization, Geneva, 2018.
- 4 E. H. Yoo and S. Y. Lee, *Sensors*, 2010, **10**, 4558–4576.
- 5 Z. Huang, S. Hu, Y. Xiong, H. Wei, H. Xu, H. Duan and W. Lai, *TrAC, Trends Anal. Chem.*, 2019, **114**, 151–170.
- 6 W. Putzbach and N. J. Ronkainen, *Sensors*, 2013, **13**, 4811–4840.
- 7 J. Lei and H. Ju, *Chem. Soc. Rev.*, 2012, **41**, 2122.
- 8 C. Zhu, G. Yang, H. Li, D. Du and Y. Lin, *Anal. Chem.*, 2015, **87**, 230–249.
- 9 S. Campuzano, P. Yáñez-Sedeño and J. M. Pingarrón, *ChemElectroChem*, 2019, **6**, 60–72.
- 10 World Health Organization, *Model List of Essential In Vitro Diagnostics*, WHO Press, 2018, p. 35.
- 11 T. S. Crofts, A. J. Gasparrini and G. Dantas, *Nat. Rev. Microbiol.*, 2017, **15**, 422–434.
- 12 J. Wang, J. Chen and S. Sen, *J. Cell. Physiol.*, 2016, **231**, 25–30.
- 13 R. E. Drury, D. O'Connor and A. J. Pollard, *Front. Immunol.*, 2017, **8**, 1182.
- 14 Y. Peng and C. M. Croce, *Signal Transduction Targeted Ther.*, 2016, **1**, 15004.
- 15 S. Kelley, E. M. Boon, J. K. Barton, N. M. Jackson and M. G. Hill, *Nucleic Acids Res.*, 1999, **27**, 4830–4837.
- 16 S. Karkare and D. Bhatnagar, *Appl. Microbiol. Biotechnol.*, 2006, **71**, 575–586.
- 17 E. E. Ferapontova, *Annu. Rev. Anal. Chem.*, 2018, **11**, 197–218.
- 18 G. L. Igloi, *Proc. Natl. Acad. Sci. U. S. A.*, 1998, **95**, 8562–8567.
- 19 Y. Seok Kim, N. H. Ahmad Raston and M. Bock Gu, *Biosens. Bioelectron.*, 2016, **76**, 2–19.
- 20 E. N. Brody and L. Gold, *Rev. Mol. Biotechnol.*, 2000, **74**, 5–13.
- 21 Y. Xiao, V. Pavlov, T. Niazov, A. Dishon, M. Kotler and I. Willner, *J. Am. Chem. Soc.*, 2004, **126**, 7430–7431.
- 22 E. Paleček, M. Fojta, M. Tomschik and J. Wang, *Biosens. Bioelectron.*, 1998, **13**, 621–628.
- 23 W. Zhou, R. Saran and J. Liu, *Chem. Rev.*, 2017, **117**, 8272–8325.
- 24 Y. Zhao, F. Chen, Q. Li, L. Wang and C. Fan, *Chem. Rev.*, 2015, **115**, 12491–12545.



25 Y. Du and S. Dong, *Anal. Chem.*, 2017, **89**, 189–215.

26 A. J. Bard and L. R. Faulkner, *Electrochemical methods : fundamentals and applications*, Wiley, 2001.

27 A. Chen and B. Shah, *Anal. Methods*, 2013, **5**, 2158.

28 J. G. Osteryoung and R. A. Osteryoung, *Anal. Chem.*, 1985, **57**, 101–110.

29 P. Dauphin-Ducharme and K. W. Plaxco, *Anal. Chem.*, 2016, **88**, 11654–11662.

30 A. B. Steel, T. M. Herne and M. J. Tarlov, *Anal. Chem.*, 1998, **70**, 4670–4677.

31 E. E. Ferapontova and E. Domínguez, *Electroanalysis*, 2003, **15**, 629–634.

32 I. Mannelli, M. Minunni, S. Tombelli, R. Wang, M. Michela Spiriti and M. Mascini, *Bioelectrochemistry*, 2005, **66**, 129–138.

33 C. J. Murphy, M. R. Arkin, Y. Jenkins, N. D. Ghatlia, S. H. Bossmann, N. J. Turro and J. K. Barton, *Science*, 1993, **262**, 1025–1029.

34 R. Tevatis, A. Prasad and R. F. Saraf, *Anal. Chem.*, 2019, **91**, 10501–10508.

35 L. Kékedy-Nagy, S. Shipovskov and E. E. Ferapontova, *Electrochim. Acta*, 2019, **318**, 703–710.

36 A. R. Arnold, M. A. Grodick and J. K. Barton, *Cell Chem. Biol.*, 2016, **23**, 183–197.

37 P. Dauphin-Ducharme, N. Arroyo-Currás and K. W. Plaxco, *J. Am. Chem. Soc.*, 2019, **141**, 1304–1311.

38 Y. Wu, R. D. Tilley and J. J. Gooding, *J. Am. Chem. Soc.*, 2019, **141**, 1162–1170.

39 J. J. Gooding and K. Gaus, *Angew. Chem., Int. Ed.*, 2016, **55**, 11354–11366.

40 P. E. Sheehan and L. J. Whitman, *Nano Lett.*, 2005, **5**, 803–807.

41 P. R. Nair and M. A. Alam, *Appl. Phys. Lett.*, 2006, **88**, 233120.

42 S. J. Smith, C. R. Nemr and S. O. Kelley, *J. Am. Chem. Soc.*, 2017, **139**, 1020–1028.

43 J. Go and M. A. Alam, *Appl. Phys. Lett.*, 2009, **95**, 033110.

44 T. M. Squires, R. J. Messinger and S. R. Manalis, *Nat. Biotechnol.*, 2008, **26**, 417–426.

45 F. Jelen, M. Tomschik and E. Paleček, *J. Electroanal. Chem.*, 1997, **423**, 141–148.

46 J. Wang, X. Cai, J. Wang, C. Jonsson and E. Palecek, *Anal. Chem.*, 1995, **67**, 4065–4070.

47 M. Zhou, Y. Zhai and S. Dong, *Anal. Chem.*, 2009, **81**, 5603–5613.

48 E. E. Ferapontova, *Curr. Anal. Chem.*, 2010, **7**, 51–62.

49 F. F. Cheng, T. T. He, H. T. Miao, J. J. Shi, L. P. Jiang and J. J. Zhu, *ACS Appl. Mater. Interfaces*, 2015, **7**, 2979–2985.

50 A. Abi and E. E. Ferapontova, *Anal. Bioanal. Chem.*, 2013, **405**, 3693–3703.

51 G. Liu, Y. Wan, V. Gau, J. Zhang, L. Wang, S. Song and C. Fan, *J. Am. Chem. Soc.*, 2008, **130**, 6820–6825.

52 D. L. Bates, *Trends Biotechnol.*, 1987, **5**, 204–209.

53 M. Staiano, A. Pennacchio, A. Varriale, A. Capo, A. Majoli, C. Capacchione and S. D'Auria, *Enzymes as Sensors*, Elsevier Science, 2017, vol. 589.

54 F. Manea, F. B. Houillon, L. Pasquato and P. Scrimin, *Angew. Chem., Int. Ed.*, 2004, **43**, 6165–6169.

55 L. Gao, J. Zhuang, L. Nie, J. Zhang, Y. Zhang, N. Gu, T. Wang, J. Feng, D. Yang, S. Perrett and X. Yan, *Nat. Nanotechnol.*, 2007, **2**, 577–583.

56 J. Wu, X. Wang, Q. Wang, Z. Lou, S. Li, Y. Zhu, L. Qin and H. Wei, *Chem. Soc. Rev.*, 2019, **48**, 1004–1076.

57 C. N. Loynachan, M. R. Thomas, E. R. Gray, D. A. Richards, J. Kim, B. S. Miller, J. C. Brookes, S. Agarwal, V. Chudasama, R. A. McKendry and M. M. Stevens, *ACS Nano*, 2018, **12**, 279–288.

58 Z. Gao and Z. Yang, *Anal. Chem.*, 2006, **78**, 1470–1477.

59 H. Yang, *Curr. Opin. Chem. Biol.*, 2012, **16**, 422–428.

60 O. Niwa, *Electroanalysis*, 1995, **7**, 606–613.

61 M. R. Akanda, Y. L. Choe and H. Yang, *Anal. Chem.*, 2012, **84**, 1049–1055.

62 Y. Huang, J. Ren and X. Qu, *Chem. Rev.*, 2019, **119**, 4357–4412.

63 S. Yadav, M. K. Masud, M. N. Islam, V. Gopalan, A. K. Lam, S. Tanaka, N.-T. Nguyen, M. S. Al Hossain, C. Li, M. Y. Yamauchi and M. J. A. Shiddiky, *Nanoscale*, 2017, **9**, 8805–8814.

64 M. Kamal Masud, M. N. Islam, M. H. Haque, S. Tanaka, V. Gopalan, G. Alici, N.-T. Nguyen, A. K. Lam, M. S. A. Hossain, Y. Yamauchi and M. J. A. Shiddiky, *Chem. Commun.*, 2017, **53**, 8231–8234.

65 M. N. Islam, M. K. Masud, N. T. Nguyen, V. Gopalan, H. R. Alamri, Z. A. Alothman, M. S. Al Hossain, Y. Yamauchi, A. K. Y. Lam and M. J. A. Shiddiky, *Biosens. Bioelectron.*, 2018, **101**, 275–281.

66 L. Tian, J. Qi, O. Oderinde, C. Yao, W. Song and Y. Wang, *Biosens. Bioelectron.*, 2018, **110**, 110–117.

67 P. Munnik, P. E. de Jongh and K. P. de Jong, *Chem. Rev.*, 2015, **115**, 6687–6718.

68 X. Wu, Y. Chai, P. Zhang and R. Yuan, *ACS Appl. Mater. Interfaces*, 2015, **7**, 713–720.

69 T. Yan, L. Zhu, H. Ju and J. Lei, *Anal. Chem.*, 2018, **90**, 14493–14499.

70 J. Chen, C. Yu, Y. Zhao, Y. Niu, L. Zhang, Y. Yu, J. Wu and J. He, *Biosens. Bioelectron.*, 2017, **91**, 892–899.

71 W. Wang, T. Bao, X. Zeng, H. Xiong, W. Wen, X. Zhang and S. Wang, *Biosens. Bioelectron.*, 2017, **91**, 183–189.

72 C. Zhang, J. He, Y. Zhang, J. Chen, Y. Zhao, Y. Niu and C. Yu, *Biosens. Bioelectron.*, 2018, **102**, 94–100.

73 S. Liu, Z. Yang, Y. Chang, Y. Chai and R. Yuan, *Biosens. Bioelectron.*, 2018, **119**, 170–175.

74 P. Kumar, A. Deep and K.-H. Kim, *TrAC, Trends Anal. Chem.*, 2015, **73**, 39–53.

75 P. Ling, J. Lei, L. Zhang and H. Ju, *Anal. Chem.*, 2015, **87**, 3957–3963.

76 D. Cheng, X. Xiao, X. Li, C. Wang, Y. Liang, Z. Yu, C. Jin, N. Zhou, M. Chen, Y. Dong, Y. Lin, Z. Xie and C. Zhang, *J. Electrochem. Soc.*, 2018, **165**, B885–B892.

77 P. Ling, J. Lei and H. Ju, *Biosens. Bioelectron.*, 2015, **71**, 373–379.

78 G. M. Espallargas and E. Coronado, *Chem. Soc. Rev.*, 2018, **47**, 533.

79 L. Jiao, Y. Wang, H. L. Jiang and Q. Xu, *Adv. Mater.*, 2018, **30**, 1703663.



80 X. Zhu, F. Kou, H. Xu, Y. Han, G. Yang, X. Huang, W. Chen, Y. Chi and Z. Lin, *Sens. Actuators, B*, 2018, **270**, 263–269.

81 L. Chen, L. Sha, Y. Qiu, G. Wang, H. Jiang and X. Zhang, *Nanoscale*, 2015, **7**, 3300–3308.

82 F. Sheng, X. Zhang and G. Wang, *J. Mater. Chem. B*, 2017, **5**, 53–61.

83 F. Zhou, Y. Yao, J. Luo, X. Zhang, Y. Zhang, D. Yin, F. Gao and P. Wang, *Anal. Chim. Acta*, 2017, **969**, 8–17.

84 H. Y. Kim, J. K. Ahn, M. Il Kim, K. S. Park and H. G. Park, *Electrochem. Commun.*, 2019, **99**, 5–10.

85 A. De La Escosura-Muñiz, L. Baptista-Pires, L. Serrano, L. Altet, O. Francino, A. Sánchez and A. Merkoçi, *Small*, 2016, **12**, 205–213.

86 A. D. Castañeda, N. J. Brenes, A. Kondajji and R. M. Crooks, *J. Am. Chem. Soc.*, 2017, **139**, 7657–7664.

87 F. Lisdat and D. Schäfer, *Anal. Bioanal. Chem.*, 2008, **391**, 1555–1567.

88 Y. Peng and Z. Gao, *Anal. Chem.*, 2011, **83**, 820–827.

89 X. Li, K. Scida and R. M. Crooks, *Anal. Chem.*, 2015, **87**, 9009–9015.

90 P. Miao, B. Wang, F. Meng, J. Yin and Y. Tang, *Bioconjugate Chem.*, 2015, **26**, 602–607.

91 M. You, S. Yang, W. Tang, F. Zhang and P. He, *Biosens. Bioelectron.*, 2018, **112**, 72–78.

92 X. Jin, L. Zhou, B. Zhu, X. Jiang and N. Zhu, *Biosens. Bioelectron.*, 2018, **107**, 237–243.

93 L. Liu, Y. Chang, N. Xia, P. Peng, L. Zhang, M. Jiang, J. Zhang and L. Liu, *Biosens. Bioelectron.*, 2017, **94**, 235–242.

94 A. Ono, S. Cao, H. Togashi, M. Tashiro, T. Fujimoto, T. MacHinami, S. Oda, Y. Miyake, I. Okamoto and Y. Tanaka, *Chem. Commun.*, 2008, 4825–4827.

95 A. Rotaru, S. Dutta, E. Jentsch, K. Gothelf and A. Mokhir, *Angew. Chem., Int. Ed.*, 2010, **49**, 5665–5667.

96 P. Miao, T. Zhang, J. Xu and Y. Tang, *Anal. Chem.*, 2018, **90**, 11154–11160.

97 A. Suela-Ngam, P. D. Howes, C. E. Stanley and A. J. Demello, *ACS Sens.*, 2019, **4**, 1560–1568.

98 C. Yang, K. Shi, B. Dou, Y. Xiang, Y. Chai and R. Yuan, *ACS Appl. Mater. Interfaces*, 2015, **7**, 1188–1193.

99 Y. Wang, X. X. Zhang, L. Zhao, T. Bao, W. Wen, X. X. Zhang and S. Wang, *Biosens. Bioelectron.*, 2017, **98**, 386–391.

100 Q. Hu, W. Hu, J. Kong and X. Zhang, *Biosens. Bioelectron.*, 2015, **63**, 269–275.

101 Y. Ye, Y. Liu, S. He, X. Xu, X. Cao, Y. Ye and H. Zheng, *Sens. Actuators, B*, 2018, **272**, 53–59.

102 N. Gao, F. Gao, S. He, Q. Zhu, J. Huang, H. Tanaka and Q. Wang, *Anal. Chim. Acta*, 2017, **951**, 58–67.

103 F. Wang, Y. Chu, Y. Ai, L. Chen and F. Gao, *Microchim. Acta*, 2019, **186**, 116.

104 J. Wang, G. Liu and A. Merkoçi, *J. Am. Chem. Soc.*, 2003, **125**, 3214–3215.

105 W. Zhu, X. Su, X. Gao, Z. Dai and X. Zou, *Biosens. Bioelectron.*, 2014, **53**, 414–419.

106 X. M. Li, L. L. Wang, J. Luo and Q. L. Wei, *Biosens. Bioelectron.*, 2015, **65**, 245–250.

107 C. C. Li, J. Hu, M. Lu and C. Y. Zhang, *Biosens. Bioelectron.*, 2018, **122**, 51–57.

108 B. Kaur, K. Malecka, D. A. Cristaldi, C. S. Chay, I. Mames, H. Radecka, J. Radecki and E. Stulz, *Chem. Commun.*, 2018, **54**, 11108–11111.

109 I. Grabowska, D. G. Singleton, A. Stachyra, A. Góra-Sochacka, A. Sirko, W. Zagórski-Ostoja, H. Radecka, E. Stulz and J. Radecki, *Chem. Commun.*, 2014, **50**, 4196–4199.

110 L. Wang, R. Ma, L. Jiang, L. Jia, W. Jia and H. Wang, *Biosens. Bioelectron.*, 2017, **92**, 390–395.

111 P. Jolly, M. R. Batistuti, A. Miodek, P. Zhurauski, M. Mulato, M. A. Lindsay and P. Estrela, *Sci. Rep.*, 2016, **6**, 36719.

112 Y. H. Yuan, Y. Di Wu, B. Z. Chi, S. H. Wen, R. P. Liang and J. D. Qiu, *Biosens. Bioelectron.*, 2017, **97**, 325–331.

113 K. Deng, X. Liu, C. Li and H. Huang, *Biosens. Bioelectron.*, 2018, **117**, 168–174.

114 D. Gong, X. Hui, Z. Guo and X. Zheng, *Talanta*, 2019, **198**, 534–541.

115 M. Chen, N. Gan, T. Li, Y. Wang, Q. Xu and Y. Chen, *Anal. Chim. Acta*, 2017, **968**, 30–39.

116 S. Huang, N. Gan, T. Li, Y. Zhou, Y. Cao and Y. Dong, *Talanta*, 2018, **179**, 28–36.

117 J. Chang, X. Wang, J. Wang, H. Li and F. Li, *Anal. Chem.*, 2019, **91**, 3604–3610.

118 H. F. Cui, T. Bin Xu, Y. L. Sun, A. W. Zhou, Y. H. Cui, W. Liu and J. H. T. Luong, *Anal. Chem.*, 2015, **87**, 1358–1365.

119 X. Miao, Z. Li, A. Zhu, Z. Feng, J. Tian and X. Peng, *Biosens. Bioelectron.*, 2016, **83**, 39–44.

120 S. Yu, Y. Wang, L. P. Jiang, S. Bi and J. J. Zhu, *Anal. Chem.*, 2018, **90**, 4544–4551.

121 D. Zhu, W. Liu, W. Cao, J. Chao, S. Su, L. Wang and C. Fan, *Electroanalysis*, 2018, **30**, 1349–1356.

122 R. Tavallaie, J. McCarroll, M. Le Grand, N. Ariotti, W. Schuhmann, E. Bakker, R. D. Tilley, D. B. Hibbert, M. Kavallaris and J. J. Gooding, *Nat. Nanotechnol.*, 2018, **13**, 1066–1071.

123 J. Tang and D. Tang, *Microchim. Acta*, 2015, **182**, 2077–2089.

124 J. M. George, A. Antony and B. Mathew, *Microchim. Acta*, 2018, **185**, 358.

125 H. Huang and J.-J. Zhu, *Analyst*, 2013, **138**, 5855.

126 F. Zhao, T. Sun, F. Geng, P. Chenand and Y. Gao, *Int. J. Electrochem. Sci.*, 2019, **14**, 5287–5304.

127 J. Tang and D. Tang, *Microchim. Acta*, 2015, **182**, 2077–2089.

128 L. D. Burke and P. F. Nugent, *Gold Bull.*, 1997, **30**, 43–53.

129 H. Cai, Y. Xu, N. Zhu, P. He and Y. Fang, *Analyst*, 2002, **127**, 803–808.

130 M. Hasanzadeh, N. Shadjou and M. de la Guardia, *TrAC, Trends Anal. Chem.*, 2015, **72**, 1–9.

131 C. Xu and X. Qu, *NPG Asia Mater.*, 2014, **6**, e90.

132 G. Yang, C. Zhu, D. Du, J. Zhu and Y. Lin, *Nanoscale*, 2015, **7**, 14217–14231.

133 C.-J. Shih, *Chimia*, 2016, **70**, 800–804.

134 J. Chen, C. Yu, Y. Zhao, Y. Niu, L. Zhang, Y. Yu, J. Wu and J. He, *Biosens. Bioelectron.*, 2017, **91**, 892–899.

135 K. J. Land, D. I. Boeras, X. S. Chen, A. R. Ramsay and R. W. Peeling, *Nat. Microbiol.*, 2019, **4**, 46–54.



136 C. S. Wood, M. R. Thomas, J. Budd, T. P. Mashamba-Thompson, K. Herbst, D. Pillay, R. W. Peeling, A. M. Johnson, R. A. McKendry and M. M. Stevens, *Nature*, 2019, **566**, 467–474.

137 D. T. Chiu, A. J. deMello, D. Di Carlo, P. S. Doyle, C. Hansen, R. M. Maceiczyk and R. C. R. Wootton, *Chem*, 2017, **2**, 201–223.

138 P. A. Aurooux, Y. Koc, A. DeMello, A. Manz and P. J. R. Day, *Lab Chip*, 2004, **4**, 534–546.

139 A. J. De Mello, *Lab Chip*, 2001, **1**, 24N.

140 D. G. Rackus, M. H. Shamsi and A. R. Wheeler, *Chem. Soc. Rev.*, 2015, **5320**, 5320.

141 K. Yamada, H. Shibata, K. Suzuki and D. Citterio, *Lab Chip*, 2017, **17**, 1206–1249.

142 World Health Organization, *WHO list of prequalified diagnostic products*, Geneva, 2019.

143 W. Dungchai, O. Chailapakul and C. S. Henry, *Anal. Chem.*, 2009, **81**, 5821–5826.

144 K. Yamanaka, M. C. Vestergaard and E. Tamiya, *Sensors*, 2016, **16**, 1761.

145 C. T. Kokkinos, D. L. Giokas, A. S. Economou, P. S. Petrou and S. E. Kakabakos, *Anal. Chem.*, 2018, **90**, 13.

146 W. R. de Araujo, C. M. R. Frasson, W. A. Ameku, J. R. Silva, L. Angnes and T. R. L. C. Paixão, *Angew. Chem., Int. Ed.*, 2017, **56**, 15113–15117.

147 J. C. Cunningham, N. J. Brenes and R. M. Crooks, *Anal. Chem.*, 2014, **86**, 6166–6170.

148 K. Scida, J. C. Cunningham, C. Renault, I. Richards and R. M. Crooks, *Anal. Chem.*, 2014, **86**, 6501–6507.

149 M.-N. Tsagloglou, A. Nemiroski, G. Camci-Unal, D. C. Christodouleas, L. P. Murray, J. T. Connelly and G. M. Whitesides, *Anal. Biochem.*, 2018, **543**, 116–121.

150 K. Hsieh, A. S. Patterson, B. S. Ferguson, K. W. Plaxco and H. T. Soh, *Angew. Chem., Int. Ed.*, 2012, **51**, 4896–4900.

151 M. Zhou and S. Dong, *Acc. Chem. Res.*, 2011, **44**, 1232–1243.

152 Metrohm, Portable potentiostats, <http://www.metrohm-autolab.com/Products/Echem/PortablePot/> PortablePotentiostats.html, (accessed 11 August 2019).

153 BioLogic Science Instruments, Portable potentiostat, [http://www.bio-logic.net/en/products/potentiostatgalvanostat-eis/pg581-portable-potentiostatgalvanostat/](http://www.bio-logic.net/en/products/potentiostat-galvanostat-eis/pg581-portable-potentiostatgalvanostat/), (accessed 11 August 2019).

154 PalmSens Compact Electrochemical Interfaces, EmStat, <https://www.palmsens.com/product/emstat/>, (accessed 11 August 2019).

155 A. Nemiroski, D. C. Christodouleas, J. W. Hennek, A. A. Kumar, E. J. Maxwell, M. T. Fernández-Abedul, G. M. Whitesides, M. T. Fernandez-Abedul and G. M. Whitesides, *Proc. Natl. Acad. Sci. U. S. A.*, 2014, **111**, 11984–11989.

156 A. Ainla, M. P. S. Mousavi, M. N. Tsagloglou, J. Redston, J. G. Bell, M. T. Fernández-Abedul and G. M. Whitesides, *Anal. Chem.*, 2018, **90**, 6240–6246.

157 Z. W. She, J. Kibsgaard, C. F. Dickens, I. Chorkendorff, J. K. Nørskov and T. F. Jaramillo, *Science*, 2017, **355**, eaad4998.

158 E. Pastor, F. Le Formal, M. T. Mayer, S. D. Tilley, L. Francàs, C. A. Mesa, M. Grätzel and J. R. Durrant, *Nat. Commun.*, 2017, **8**, 14280.

159 S. Geiger, O. Kasian, M. Ledendecker, E. Pizzutilo, A. M. Mingers, W. T. Fu, O. Diaz-Morales, Z. Li, T. Oellers, L. Fruchter, A. Ludwig, K. J. J. Mayrhofer, M. T. M. Koper and S. Cherevko, *Nat. Catal.*, 2018, **1**, 508–515.

160 S. Fatayer, F. Albrecht, Y. Zhang, D. Urbonas, D. Peña, N. Moll and L. Gross, *Science*, 2019, **365**, 142–145.

161 Y. Li, S. Li, J. Wang and G. Liu, *Trends Biotechnol.*, 2019, **37**, 730–743.

162 J. S. Gootenberg, O. O. Abudayyeh, J. W. Lee, P. Essletzbichler, A. J. Dy, J. Joung, V. Verdine, N. Donghia, N. M. Daringer, C. A. Freije, C. Myhrvold, R. P. Bhattacharya, J. Livny, A. Regev, E. V. Koonin, D. T. Hung, P. C. Sabeti, J. J. Collins and F. Zhang, *Science*, 2017, **356**, 438–442.

163 J. S. Gootenberg, O. O. Abudayyeh, M. J. Kellner, J. Joung, J. J. Collins and F. Zhang, *Science*, 2018, **360**, 439–444.

164 C. Myhrvold, C. A. Freije, J. S. Gootenberg, O. O. Abudayyeh, H. C. Metsky, A. F. Durbin, M. J. Kellner, A. L. Tan, L. M. Paul, L. A. Parham, K. F. Garcia, K. G. Barnes, B. Chak, A. Mondini, M. L. Nogueira, S. Isern, S. F. Michael, I. Lorenzana, N. L. Yozwiak, B. L. MacInnis, I. Bosch, L. Gehrke, F. Zhang and P. C. Sabeti, *Science*, 2018, **360**, 444–448.

165 R. Hajian, S. Balderston, T. Tran, T. deBoer, J. Etienne, M. Sandhu, N. A. Wauford, J. Y. Chung, J. Nokes, M. Athaiya, J. Paredes, R. Peytavi, B. Goldsmith, N. Murthy, I. M. Conboy and K. Aran, *Nat. Biomed. Eng.*, 2019, **3**, 427–437.

166 M. Díaz-González, X. Muñoz-Berbel, C. Jiménez-Jorquera, A. Baldi and C. Fernández-Sánchez, *Electroanalysis*, 2014, **26**, 1154–1170.

167 A. Hassibi, A. Manickam, R. Singh, S. Bolouki, R. Sinha, K. B. Jirage, M. W. McDermott, B. Hassibi, H. Vikalo, G. Mazarei, L. Pei, L. Bousse, M. Miller, M. Heshami, M. P. Savage, M. T. Taylor, N. Gagini, N. Wood, P. Mantina, P. Grogan, P. Kuimelis, P. Savalia, S. Conradson, Y. Li, R. B. Meyer, E. Ku, J. Ebert, B. A. Pinsky, G. Dolganov, T. Van, K. A. Johnson, P. Naraghi-Arani, R. G. Kuimelis and G. Schoolnik, *Nat. Biotechnol.*, 2018, **36**, 738–745.

168 S. Goodwin, J. D. McPherson and W. R. McCombie, *Nat. Rev. Genet.*, 2016, **17**, 333–351.

169 ‘Oxford Nanopore Technologies’ MinION, <https://nanoporetech.com/products/minion>, (accessed 4 August 2019).

170 S. Saini, *Cell. Oncol.*, 2016, **39**, 97–106.

171 K. K. Jain, *The Handbook of Biomarkers*, Springer New York, New York, NY, 2017.

172 S. Wang, L. Zhang, S. Wan, S. Cansiz, C. Cui, Y. Liu, R. Cai, C. Hong, I. T. Teng, M. Shi, Y. Wu, Y. Dong and W. Tan, *ACS Nano*, 2017, **11**, 3943–3949.

173 V. Gligorijević, N. Malod-Dognin and N. Pržulj, *Proteomics*, 2016, **16**, 741–758.

174 R. W. Peeling and D. Mabey, *Clin. Microbiol. Infect.*, 2010, **16**, 1062–1069.

175 FIND, Target product profiles, <https://www.finddx.org/target-product-profiles/>, (accessed 4 August 2019).

